

# MDDC Multi-Length Scale Data Architecture Contribution Report – PNNL, INL, ANL, LANL and ORNL

September 2023

Mohammad Fuad Nur Taufique (PNNL)  
Isabella Van Rooyen (PNNL)  
Sudipta Biswas (INL)  
Michael McMurtrey (INL)  
Mathew Swisher (INL)  
Mark Messner (ANL)  
Srinivas Aditya Mantri (ANL)  
Michael Brandt (LANL)  
Bryant Kanies (LANL)

Ayoub Soulami (PNNL)  
Andrea Jokisaari (INL)  
William Chuirazzi (INL)  
Stephanie Pitts (INL)  
W. Tanner Yorgason (INL)  
Tianchen Hu (ANL)  
Xuan Zhang (ANL)  
Laurent Capolungo (LANL)  
Vincent C. Paquit (ORNL)

## DISCLAIMER

This report was prepared as an account of work sponsored by an agency of the United States Government. Neither the United States Government nor any agency thereof, nor Battelle Memorial Institute, nor any of their employees, makes **any warranty, express or implied, or assumes any legal liability or responsibility for the accuracy, completeness, or usefulness of any information, apparatus, product, or process disclosed, or represents that its use would not infringe privately owned rights.** Reference herein to any specific commercial product, process, or service by trade name, trademark, manufacturer, or otherwise does not necessarily constitute or imply its endorsement, recommendation, or favoring by the United States Government or any agency thereof, or Battelle Memorial Institute. The views and opinions of authors expressed herein do not necessarily state or reflect those of the United States Government or any agency thereof.

PACIFIC NORTHWEST NATIONAL LABORATORY  
*operated by*  
BATTELLE  
*for the*  
UNITED STATES DEPARTMENT OF ENERGY  
*under Contract DE-AC05-76RL01830*

Printed in the United States of America

Available to DOE and DOE contractors from  
the Office of Scientific and Technical Information,  
P.O. Box 62, Oak Ridge, TN 37831-0062

[www.osti.gov](http://www.osti.gov)  
ph: (865) 576-8401  
fox: (865) 576-5728  
email: [reports@osti.gov](mailto:reports@osti.gov)

Available to the public from the National Technical Information Service  
5301 Shawnee Rd., Alexandria, VA 22312  
ph: (800) 553-NTIS (6847)  
or (703) 605-6000  
email: [info@ntis.gov](mailto:info@ntis.gov)  
Online ordering: <http://www.ntis.gov>

# **MDDC Multi-Length Scale Data Architecture Contribution Report – PNNL, INL, ANL, LANL and ORNL**

September 2023

Mohammad Fuad Nur Taufique (PNNL)  
Isabella Van Rooyen (PNNL)  
Sudipta Biswas (INL)  
Michael McMurtrey (INL)  
Mathew Swisher (INL)  
Mark Messner (ANL)  
Srinivas Aditya Mantri (ANL)  
Michael Brandt (LANL)  
Bryant Kanies (LANL)

Ayoub Soulami (PNNL)  
Andrea Jokisaari (INL)  
William Chuirazzi (INL)  
Stephanie Pitts (INL)  
W. Tanner Yorgason (INL)  
Tianchen Hu (ANL)  
Xuan Zhang (ANL)  
Laurent Capolungo (LANL)  
Vincent C. Paquit (ORNL)

Prepared for  
the U.S. Department of Energy  
under Contract DE-AC05-76RL01830

Pacific Northwest National Laboratory  
Richland, Washington 99354

## Abstract

This report offers a comprehensive view of data streams currently generated at Pacific Northwest National Laboratory, Idaho National Laboratory, Argonne National Laboratory, Los Alamos National Laboratory, and Oak Ridge National Laboratory set to integrate into the evolving Multi-Dimensional Data Correlation framework at Oak Ridge National Laboratory. Developed by the Advanced Materials and Manufacturing Technologies program, the Multi-Dimensional Data Correlation framework serves as a cutting-edge software to manage data relevant to advanced manufacturing and material behavior in advanced reactors. The report defines data streams, highlights their generation methods and visualization methods both for experimental and computational aspects relevant to the Advanced Materials and Manufacturing Technologies project. A logical next step for this work is to integrate the MDDC framework into PNNL's, INL's, ANL's, LANL's and ORNL's fabrication, experimentation, and modelling workflows. This would require setting up the MDDC framework at PNNL, INL, ANL, and LANL and integrating it into the data collection and storage for these different activities.

## Acknowledgments

The research presented here was supported by the Advanced Materials and Manufacturing Technology (AMMT) program of the DOE Office of Nuclear Energy. PNNL is a multi-program national laboratory operated for the U.S. Department of Energy (DOE) by Battelle Memorial Institute under Contract No. DE-AC05-76RL01830.

## Acronyms and Abbreviations

AMMT	Advanced Materials and Manufacturing Technologies
ANL	Argonne National Laboratory
APS	Advanced Photon Source
ATR	Advanced Test Reactor
DDD	discrete dislocation dynamics
FEM	finite element method
HEDM	high energy diffraction microscopy
HPC	high-performance computing
INL	Idaho National Laboratory
LAMMPS	Large-scale Atomic/Molecular Massively Parallel Simulator
LApX	Los Alamos Polycrystal (code)
MDDC	Multi-Dimensional Data Correlation
ORS	Object Research Systems
pdf	portable document file
PNNL	Pacific Northwest National Laboratory
SEM	scanning electron microscopy
ShAPE	Shear Assisted Extrusion and Processing
SPH	Smoothed Particle Hydrodynamics
SSD	Silicon Drift Detector
STEM	scanning transmission electron microscopy
TEM	transmission electron microscopy
VASP	Vienna Ab Initio Simulation Package

## Contents

Abstract.....	ii
Acknowledgments.....	iii
Acronyms and Abbreviations.....	iv
1.0 Introduction .....	1
2.0 Experimental Equipment and Simulation Tools: PNNL .....	2
2.1 Advanced Manufacturing Equipment.....	2
2.1.1 Shear Assisted Extrusion and Processing (ShAPE).....	2
2.1.2 Xplore Micro Compounder .....	3
2.1.3 Custom Built Fused Filament Fabrication Printer .....	4
2.1.4 Particle Size Analyzer.....	6
2.2 Mechanical Testing and Characterization Equipment.....	7
2.2.1 JEOL ARM200CF S/TEM .....	7
2.2.2 Transmission Electron Microscopy (TEM) .....	8
2.2.3 Scanning Electron Microscopy (SEM).....	10
2.2.4 Microhardness Tester .....	11
2.2.5 X-ray Diffractometer – D8 Discover by Bruker .....	12
2.2.6 Sonix Fusion Acoustic Microscope .....	13
2.2.7 Gas Pycnometer.....	14
2.2.8 Digital Microscope .....	15
2.3 Heat Treatment Equipment .....	16
2.3.1 Furnaces .....	16
2.4 Materials Modeling Tool.....	17
2.4.1 ANSYS LS-DYNA Software .....	17
2.4.2 Thermo-Calc 2000b Software .....	18
3.0 Experimental Equipment and Simulation Tools: INL .....	20
3.1 Mechanical Testing and Characterization Equipment.....	20
3.1.1 ZEISS XRadia 520 Versa .....	20
3.1.2 Servo-hydraulic load frames .....	21
3.1.3 Electro-mechanical Load Frames .....	23
3.1.4 Static Load Frames .....	24
3.1.5 Hardness Testing .....	26
3.1.6 Optical Microscopes .....	27
3.1.7 Electron Microscopes .....	29
3.1.8 Neutron Irradiation Testing .....	30
3.2 Heat Treatment Equipment .....	31
3.2.1 Furnaces .....	31
3.3 Materials Modeling Tool .....	33

3.3.1	LAMMPS .....	33
3.3.2	Vienna Ab Initio Simulation Package (VASP) .....	35
3.3.3	Multiphysics Object-Oriented Simulation Environment (MOOSE) .....	37
3.3.4	MARMOT .....	40
3.3.5	Data Collection and Transfer, Metadata, and Data Visualization and Analysis .....	41
4.0	Experimental Equipment and Simulation Tools: ANL.....	42
4.1	Advanced Manufacturing Equipment.....	42
4.1.1	Renishaw AM 400 .....	42
4.1.2	BeAM Modulo 250 .....	43
4.2	Mechanical Testing and Characterization Equipment.....	44
4.2.1	Instron Servo-Hydraulic Load Frames .....	44
4.2.2	Direct Load and Lever Arm Creep Frames .....	45
4.2.3	Various Box and Tube Furnaces .....	46
4.2.4	Hysitron TI Premier Nanoindenter .....	47
4.2.5	Buehler Indenter.....	48
4.2.6	FEI Talos TEM .....	49
4.2.7	JEOL JSM-IT800 SEM .....	50
4.2.8	The Advanced Photon Source (APS).....	51
4.2.9	High Energy Diffraction Microscopy .....	53
4.3	Materials Modeling Tool.....	54
4.3.1	Macrostructural Modeling for Residual Stress and Distortion .....	54
4.3.2	Microstructural Modeling for Material Properties .....	55
4.4	Geometric Relational Database .....	56
4.4.1	Overview of GeomDB.....	57
4.4.2	Software design.....	57
4.4.3	Mesh and voxelization .....	57
4.4.4	Locations.....	58
4.4.5	Conditions .....	60
4.4.6	Properties.....	60
4.4.7	Database.....	61
4.4.8	Checkpointing.....	62
4.4.9	Example 1: Single Geometry Relation Database – The Basic Workflow .....	63
4.4.10	Example 2. Replicated-Geometry Relational Database –Real Data with Machine Learning .....	65
5.0	Experimental Equipment and Simulation Tools: LANL.....	68
5.1	Advanced Manufacturing Equipment.....	68
5.1.1	EOS 400 M 400.....	68

5.1.2	Data Collection and Transfer .....	68
5.1.3	Data Visualization and Analysis .....	68
5.1.4	EOS 400 M 290 .....	69
5.2	Mechanical Testing and Materials Characterization Equipment .....	70
5.2.1	Creep Testing .....	70
5.2.2	Mechanical Testing: Tension and Compression 1 .....	71
5.2.3	Mechanical Testing: Tension and Compression 2 .....	72
5.2.4	Mechanical Properties Characterization at High Temperature .....	74
5.2.5	Microstructure Characterization: Scanning Electron Microscope 1 .....	75
5.2.6	Microstructure Characterization: Scanning Electron Microscope 2 .....	76
5.3	Materials Modeling Tool .....	77
5.3.1	Micron-scale Simulations .....	77
5.3.2	Thermodynamic Simulations .....	78
5.3.3	Polycrystal Plasticity Simulations: LApX .....	79
5.3.4	Surrogate Models: LAROMance .....	81
6.0	Experimental Equipment and Simulation Tools: ORNL .....	83
6.1	Advanced Manufacturing Technologies .....	83
6.1.1	Renishaw AM 250 .....	83
6.2	Mechanical Testing and Material characterization Equipment .....	88
6.2.1	X-Ray Computed Tomography: METROTOM .....	88
6.2.2	XRADA VERSA 620 .....	89
7.0	Conclusions and Recommendations .....	92
8.0	References .....	93

## Figures

Figure 1.	Shear Assisted Processing and Extrusion (ShAPE) Machine.....	2
Figure 2.	Example Extrudate Geometries Produced Using ShAPE .....	2
Figure 3.	Xplore MC 15 HT compounder.....	3
Figure 4.	Custom FFF Printer .....	5
Figure 5.	Malvern MS2000 and Microtrac Sync M5000 Particle Size analyzers .....	6
Figure 6.	JEOL ARM200CF Aberration Corrected Microscope .....	7
Figure 7.	GranArm STEM in the Radiochemical Processing Laboratory at PNNL .....	9
Figure 8.	Helios Hydra Plasma FIB in the ESC Building.....	10
Figure 9.	Microhardness Tester CM-802AT, Sun-Tec Corporation in PNNL's 3410 Building.....	11
Figure 10.	D8 Discover Powder X-Ray Diffractometer in the LSL2 Building .....	12
Figure 11.	Sonix Fusion Scanning Acoustic Microscope .....	13
Figure 12.	Micromeritics AccuPyc 1340 II .....	14
Figure 13.	Keyence VHX-7020 Digital Microscope.....	15
Figure 14.	Furnace CM H <sub>2</sub> Furnace Model 1516GSH2FL.....	16
Figure 15.	ZEISS Xradia 520 Versa X-ray Microscope.....	20
Figure 16.	Typical MTS Servo-Hydraulic Load Frame at INL .....	22
Figure 17.	Typical Electro-Mechanical Load Frame at INL.....	23
Figure 18.	Typical Static Load Frame at INL .....	25
Figure 19.	Rockwell Hardness Indenter (left) and Vickers Indenter (right) at INL .....	26
Figure 20.	Typical Optical Microscope at INL.....	28
Figure 21.	Quanta FEG 650 SEM at INL.....	29
Figure 22.	Typical Box Furnace Set-Up at INL.....	32
Figure 23.	Early Stage of a Collision Cascade in Fe-Cr-Ni (red, blue, and yellow, respectively) Simulated by Molecular Dynamics Using LAMMPS and Visualized Using OVITO .....	33
Figure 24.	Representation of an Fe-Cr-Ni System Calculated by VASP and Visualized with VESTA.....	35
Figure 25.	Logo of the MOOSE Framework from INL.....	37
Figure 26.	Metadata from a MOOSE Simulation, Demonstrating the Type of Information to be Collected with a Mechanics Simulation Example .....	39
Figure 27.	ANL's Renishaw AM 400 Powder Bed Fusion Machine .....	42
Figure 28.	ANL's BeAM Modulo 250 Directed Energy Deposition Printer .....	43
Figure 29.	An ANL Servo-Hydraulic Load Frame with the Furnace Open .....	44
Figure 30.	Direct Load Creep Frames.....	45
Figure 31.	Lever Arm Creep Frames.....	46
Figure 32.	Some of ANL's Box Furnaces .....	47
Figure 33.	Hysitron TI Premier Nanoindenter .....	47

Figure 34.	Buehler Indenter .....	48
Figure 35.	One of ANL's Optical Microscopes .....	49
Figure 36.	Talos Scanning Transmission Electron Microscope in ANL's Center for Nanoscale Materials .....	50
Figure 37.	JEOL JSM-IT800 SEM in ANL's Center for Nanoscale Materials .....	51
Figure 38.	Schematics Showing the Principle of the Wide-Angle X-Ray Scattering Technique Data Collection and Data Processing .....	52
Figure 39.	Single Tomography Image from a Stack .....	52
Figure 40.	Reconstructed Tomography Dataset (as an STL file) Showing Internal Porosity in a Sample .....	53
Figure 41.	Visualization of a Near Field HEDM Dataset as a Point Cloud of IPF Mapped Grain Orientations .....	54
Figure 42.	Example Residual Stress Simulation (here of a weld) Showing Temperature on the Left and Residual Strain on the Right .....	55
Figure 43.	Typical Crystal Plasticity Finite Element Method Simulation of a Composite Material. The fringe colors show the local stress in the loading direction. ....	56
Figure 44.	Voxelation of the Stanford Bunny with Three Different Pitches. (Left) pitch = 3, (middle) pitch = 2, (right) pitch = 1 .....	58
Figure 45.	Sub-Voxelation Construction Using (left) Points (middle) Bounding Box and (right) Plane .....	59
Figure 46.	(left) Negation of the Bounding Box (middle); Intersection of the Bounding Box and the Plane; and (right) Union of the Bounding Box and the Points .....	60
Figure 47.	Data Structures of (left) Single-Geometry Relational Database and (right) Replicated-Geometry Relational Database .....	62
Figure 48.	Example 1 Query Result .....	64
Figure 49.	Example 2: Experimental Data and Model Predictions .....	67
Figure 50.	Example 2: Validation of the Inferred Statistical Model Against the 48 Unseen Data Points .....	67
Figure 51.	EOS M400-1 3-D Printer .....	68
Figure 52.	EOS M400-1 3-D Printer .....	69
Figure 53.	Zwick Roll Creep Testing Machine .....	70
Figure 54.	MTS Electromechanical Load Frame .....	71
Figure 55.	MTS Criterion 43 electromechanical load frame .....	73
Figure 56.	Gleeble 1500 .....	74
Figure 57.	JEOL JSM-IT 100 Scanning Electron Microscope .....	75
Figure 58.	Environmental Scanning Electron Microscope Equipped with Several Detectors (ETD, CBS, ABS, GSED, LVD) .....	76
Figure 59.	Example of Microstructure Configuration Generated by DDD. The specific configuration shown corresponds to a small grain polycrystal containing dislocation lines and precipitates (size ~10nm). ....	77
Figure 60.	Experimental Time Temperature Precipitation Diagram for 316L Steel. The tool under development will produce similar plots as shown here. ....	79

Figure 61.	Constitutive Modeling Modules Available within LApX .....	80
Figure 62.	Predicted Envelope of the Steady State Creep Rate of 316H Processed by AM. Temperature is 650°C. The microstructure was varied as a function of precipitate size and density, dislocation content, porosity and grain aspect ratio. ....	80
Figure 63.	Computational Flowchart Showing How LAROMance Models are Developed.....	82
Figure 64.	RenishawAM250-008W73 Single-Laser, Laser Powder Bed Fusion Printer .....	83
Figure 65.	Peregrine Metadata Manager for the Renishaw AM 250 .....	85
Figure 66.	RenishawAM250-008W73 .....	88
Figure 67.	XRADA VERSA 620 .....	90

## Tables

Table 1.	Description of the Data Volume, Associated Software Tools, and Other Data for the ShAPE Machine .....	3
Table 2.	Description of the data volume, associated software tools and other data for the Xplore Micro Compounder equipment.....	4
Table 3.	Description of the data volume, associated software tools and other data for the custom FFF Printer .....	5
Table 4.	Description of the data volume, associated software tools and other data for the Particle Size analyzers.....	6
Table 5.	Description of the Data Volume, Associated Software Tools and Other Data for the JEOL ARM200CF .....	7
Table 6.	Description of the Data Volume, Associated Software Tools and Other Data for the GrandArm-300F STEM Equipment.....	9
Table 7.	Description of the Data Volume, Associated Software Tools and Other Data for the SEM Equipment .....	10
Table 8.	Description of the Data Volume, Associated Software Tools and Other Data for the Equipment D8 Discover .....	12
Table 9.	Description of the Data Volume, Associated Software Tools and Other Data for the Equipment D8 Discover .....	13
Table 10.	Description of the Data Volume, Associated Software Tools and Other Data for the Sonix Fusion Scanning Acoustic Microscope.....	14
Table 11.	Description of the data volume, associated software tools and other data for the Micromeritics AccuPyc 1340 II .....	14
Table 12.	Description of the data volume, associated software tools and other data for the Keyence VHX 7020 Digital Microscope.....	16
Table 13.	Description of the data volume, associated software tools and other data for the CM H <sub>2</sub> Furnace .....	17
Table 14.	Description of Data Volume and Associated Software Tools for the SPH in LS-DYNA Software .....	17
Table 15.	Description of Data Volume and Associated Software Tools for the Thermo-Calc 2020b Software .....	19
Table 16.	Description of the Data Volume, Associated Software Tools and Other Data for the ZEISS Xradia 520 Versa X-ray Microscope Used at INL.....	20
Table 17.	Description of the Data Volume, Associated Software Tools and Other Data for a Generic MTS Servo-Hydraulic Machine at INL .....	22
Table 18.	Typical Data Collected In Tests on the Servo-Hydraulic Machines at INL .....	23
Table 19.	Description of the Data Volume, Associated Software Tools and Other Data for a Generic Electro-Mechanical Load Frame at INL .....	24
Table 20.	Typical Data Collected in Tests on the Electro-Mechanical Load Frames at INL .....	24
Table 21.	Description of The Data Volume, Associated Software Tools and Other Data for a Static Load Frame at INL.....	25
Table 22.	Typical Data Collected in Tests on the Static Load Frames at INL .....	26

Table 23.	Description of the Data Volume, Associated Software Tools and Other Data for Generic Hardness Testing at INL .....	27
Table 24.	Typical Data Collected During Hardness Testing at INL.....	27
Table 25.	Description of the Data Volume, Associated Software Tools and Other Data for a Generic Optical Microscope at INL .....	28
Table 20.	Typical Data Collected in Optical Microscopy Examination at INL.....	28
Table 27.	Description of the Data Volume, Associated Software Tools and Other Data for a Generic Electron Microscope at INL .....	29
Table 28.	Typical Data Collected in Electron Microscopy Examinations at INL .....	30
Table 29.	Description of the Data Volume, Associated Software Tools and Other Data for a Neutron Irradiation Campaign at INL .....	30
Table 30.	Typical Data Collected for Neutron Irradiations at INL that may not be within the ECAR Document.....	31
Table 31.	Description of the Data Volume, Associated Software Tools and Other Data for Furnace Testing at INL .....	32
Table 32.	Typical Data Collected in Furnace Tests at INL .....	32
Table 33.	Description of the Data Volume, Associated Software Tools, and Other Data for LAMMPS Use at INL .....	33
Table 34.	Description of the high-performance computing needs for LAMMPS use at INL.....	34
Table 35.	Metadata Table for LAMMPS Software Use at INL .....	35
Table 36.	Description of the Data Volume, Associated Software Tools and Other Data for VASP Use at INL.....	35
Table 37.	Description of the High-Performance Computing Needs for VASP Use at INL .....	36
Table 38.	Description of the Data Volume, Associated Software Tools and Other Information for MOOSE Use at INL.....	37
Table 39.	Description of the High-Performance Computing Needs for MOOSE Use at INL.....	38
Table 40.	Description of the Data Volume, Associated Software Tools and Other Data for MARMOT Use at INL.....	40
Table 41.	Data Collected for each AM Build .....	44
Table 42.	Typical Data Collected in Tests on the ANL Servo-Hydraulic Machines .....	45
Table 43.	Typical Data Collected in a Creep Test.....	46
Table 44.	Metadata Information for RenishawAM250-008W73 Single-Laser, Laser Powder Bed Fusion Printer .....	83
Table 45.	Metadata Information for Renishaw AM 250 Printer .....	86
Table 46.	Metadata Information for Renishaw AM 250 .....	89
Table 47.	Metadata Information .....	90

## 1.0 Introduction

This report outlines the potential integration of data streams originating from Pacific Northwest National Laboratory (PNNL), Idaho National Laboratory (INL), Argonne National Laboratory (ANL), Los Alamos National Laboratory (LANL) and Oak Ridge National Laboratory (ORNL) into the emerging Multi-Dimensional Data Correlation (MDDC) framework, currently under development at Oak Ridge National Laboratory. The primary purpose of the MDDC framework is to serve as a robust data management and curation platform, facilitating the storage, retrieval, and correlation of data derived from components manufactured through diverse advanced manufacturing processes under the umbrella of Advanced Materials and Manufacturing Technologies (AMMT) program. The MDDC framework is an integral part of the broader AMMT program that seeks to comprehensively investigate the behavior of novel advanced materials, including additively manufactured materials within nuclear environments. The ultimate aim is to expedite the qualification and deployment of these materials, both in existing reactor facilities and future advanced nuclear reactors. The MDDC framework is strategically designed to accommodate a wide spectrum of material manufacturing, testing, characterization, and simulation data, with the overarching objective of fostering accessibility for the development of comprehensive insights into the material processing, structure, and physical property relationship. As part of these efforts, the MDDC framework will need to be able to store and access a wide variety of data types. This report summarizes potential data streams from different labs, including a de-scription of how the data is collected, how it is stored, and the estimated amount of data storage required. The report also briefly describes the file formats typically used to describe the data sets, with a long-term view towards making commonly generated data more accessible through the MDDC framework.

Information in the report is organized as follows:

- Chapter 1.0 – Introduction
- Chapter 2.0 – Experimental Equipment and Simulation Tools: Pacific Northwest National Laboratory
- Section 3.0 – Experimental Equipment and Simulation Tools: Idaho National Laboratory
- Section 4.0 – Experimental Equipment and Simulation Tools: Argonne National Laboratory
- Section 5.0 – Experimental Equipment and Simulation Tools: Los Alamos National Laboratory
- Section 6.0 – Experimental Equipment and Simulation Tools: Oak Ridge National Laboratory
- Section 7.0 – Conclusions and Recommendations.
- Section 8.0 – References

## 2.0 Experimental Equipment and Simulation Tools: PNNL

### 2.1 Advanced Manufacturing Equipment

#### 2.1.1 Shear Assisted Extrusion and Processing (ShAPE)

##### 2.1.1.1 Overview

PNNL's first-of-its-kind ShAPE machine (Figure 1), manufactured by Bond Technologies in Elkhart, Indiana, can rotate at 200 rpm with 3,000 Nm (2,100 ft-lb) of torque while applying a 900 kN (100 ton) ram force. This machine is used to extrude materials with improved performance, reduced embodied energy, and lower carbon footprint compared to conventional extrusion. Example extrudate profiles produced using ShAPE are shown in Figure 2 and Table 1 shows typical data type and volume.



Figure 1. Shear Assisted Processing and Extrusion (ShAPE) Machine

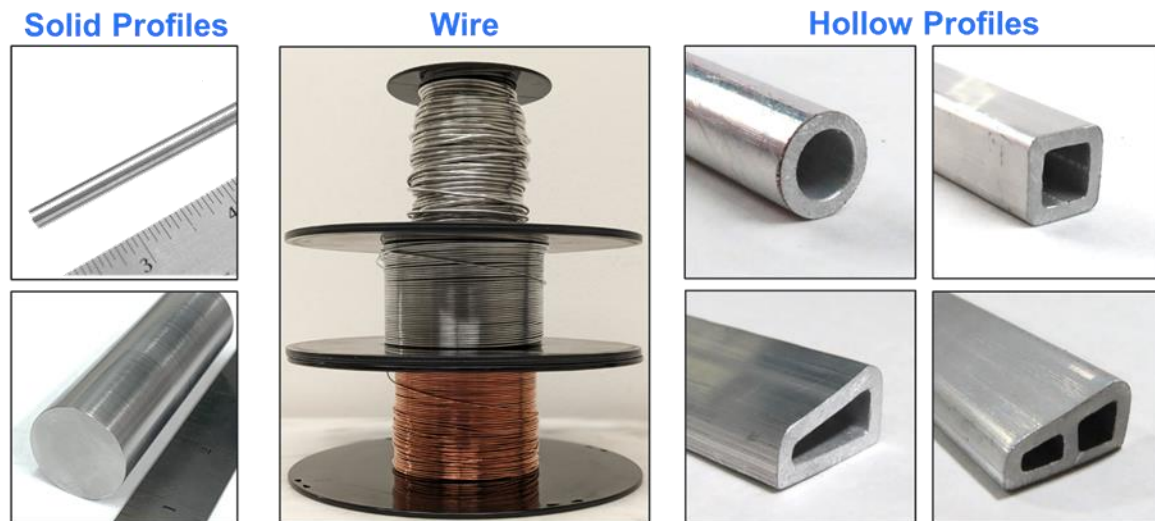


Figure 2. Example Extrudate Geometries Produced Using ShAPE

Table 1. Description of the Data Volume, Associated Software Tools, and Other Data for the ShAPE Machine

Category	Value
Digital Platform Tag(s)	Shear Assisted Processing and Extrusion; ShAPE
Digital Point of Contact	To be determined
Approximate Data Volume per Operation (GB)	To be determined
Approximate Number of Operations per Year	1,000
Associated Software Tools	Bond HMI

### 2.1.1.2 Data Collection and Transfer

Data for ram force, ram position, ram velocity, spindle torque, spindle power, and spindle rpm are logged as data files (.csv, .txt).

### 2.1.1.3 Data Visualization and Analysis

Post-processing software and methods at discretion of technical staff.

## 2.1.2 Xplore Micro Compounder

### 2.1.2.1 Overview

Xplore Micro Compounder, MC 15 HT is a 15 mL high torque compounder used to disperse, mix and extrude polymeric binders and inorganic additives (metal powders). The maximum operating temperature is 450 °C and has a screw torque of 40 Nm and a mixing rate of 1-500 rpm.



Figure 3. Xplore MC 15 HT compounder

Table 2. Description of the data volume, associated software tools and other data for the Xplore Micro Compounder equipment

Category	Value
Digital Platform Tag(s)	To be determined
Digital Point of Contact	Zachary Kennedy
Approximate Data Volume per Operation (GB)	To be determined
Approximate Number of Operations per Year	~20
Associated Software Tools	To be determined

#### 2.1.2.2 Data Collection and Transfer

Continued work needs for further development.

#### 2.1.2.3 Data Visualization and Analysis

Continued work needs for further development.

### 2.1.3 Custom Built Fused Filament Fabrication Printer

#### 2.1.3.1 Overview

A custom built FFF printer shown was used for printing with a 0.4mm stainless steel nozzle, heated bed with a PEI plate, a BondTech Extruder and E3D heater block and heat sink. Repetier Host was used as the printer interface program and a custom set of slicing parameters were set through the slicing software Slic3r.

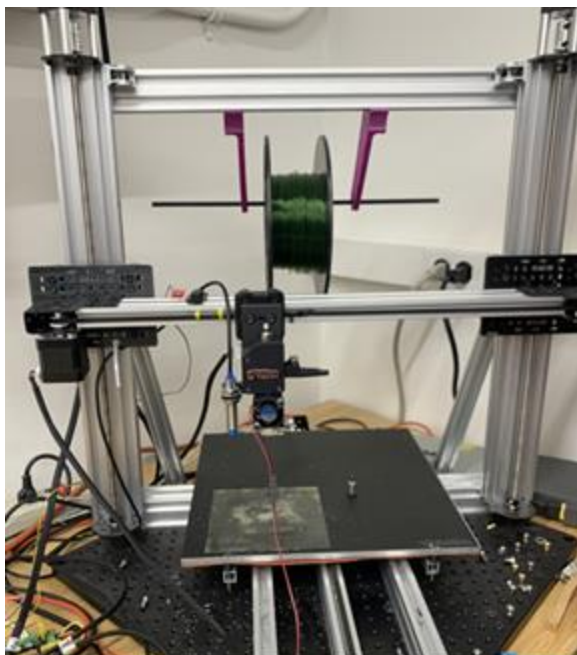


Figure 4. Custom FFF Printer

Table 3. Description of the data volume, associated software tools and other data for the custom FFF Printer

Category	Value
Digital Platform Tag(s)	To be determined
Digital Point of Contact	Michelle Fenn
Approximate Data Volume per <i>Operation</i> (GB)	6-100 KB
Approximate Number of <i>Operations</i> per Year	~200
Associated Software Tools	Slic3r

### 2.1.3.2 Data Collection and Transfer

Continued work needs for further development.

### 2.1.3.3 Data Visualization and Analysis

Continued work needs for further development

## 2.1.4 Particle Size Analyzer

### 2.1.4.1 Overview

Either a MS2000 particle size analyzer or a Microtrac Sync M5000 was used to collect particles size distribution of metal powders. Multiple dispersion units, 20, 90, 800 mL and dry powders.



Figure 5. Malvern MS2000 and Microtrac Sync M5000 Particle Size analyzers

Table 4. Description of the data volume, associated software tools and other data for the Particle Size analyzers

Category	Value
Digital Platform Tag(s)	To be determined
Digital Point of Contact	Carolyn Burns
Approximate Data Volume per Operation (GB)	~500 KB per file
Approximate Number of Operations per Year	~500
Associated Software Tools	Proprietary software from the vendor

### 2.1.4.2 Data Collection and Transfer

Particles size distribution data collected and saved in vendor supplied software. Data can be exported into a report format or to excel for further analysis.

### 2.1.4.3 Data Visualization and Analysis

Data visualization and analysis can be done in Microsoft Excel or in the instrument software.

## 2.2 Mechanical Testing and Characterization Equipment

### 2.2.1 JEOL ARM200CF S/TEM

#### 2.2.1.1 Overview

PNNL will be using scanning transmission electron microscopy (STEM) to collect an automated imaging tilt series as presented in Figure 6 and Table 5 shows the data volume and related software for this microscope. The ability to visually represent data in three dimensions provides the ability to better analyze and understand data at the nanoscale. We are developing this on the JEOL ARM200CF platform.

The JEOL ARM200CF is an atomic resolution analytical electron microscope, with a STEM Cs corrector providing a STEM-high-angle annular dark field (HAADF) resolution of 78 pm and full analytical capabilities using energy-dispersive X-ray microscopy and electron energy loss spectroscopy (EELS). The Cs-corrected electron probe has an increased current density, one order larger than conventional field-emission transmission electron microscopy, thus enabling elemental analysis at the atomic-level.

The JEOL ARM200CF provides simultaneous STEM-ABF imaging for visualizing light elements together with STEM-HAADF imaging.

Elemental EDX analysis and elemental mapping at atomic resolution is provided using twin JEOL Centurio wide area (100 mm<sup>2</sup>) silicon drift detector for high-speed and high-sensitivity detection.

The narrow energy spread that is characteristic of the cold field-emission gun enables high-energy resolution EELS analysis and fast EELS mapping with dual EELS capability using the Gatan Quantum 965ER system.

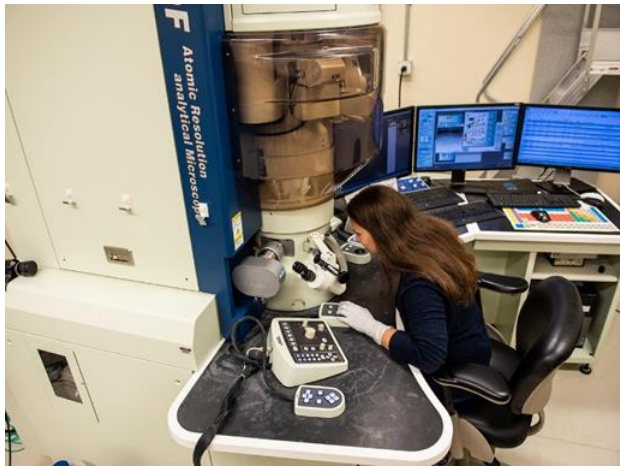


Figure 6. JEOL ARM200CF Aberration Corrected Microscope

Table 5. Description of the Data Volume, Associated Software Tools and Other Data for the JEOL ARM200CF

Category	Value
----------	-------

Digital Platform Tag(s)	To be determined
Digital Point of Contact	Matthew Olszta
Approximate Data Volume per Operation (GB)	50
Approximate Number of Operations per Year	Data can be collected daily on this microscope
Associated Software Tools	Gatan Digital Microscope Suite, JEOL TEM Center

### 2.2.1.2 Data Collection and Transfer

As part of the Computer Vision work package, we are collecting automated STEM tilt series. The procedure consists of locating a single feature and tilting it across an angular range of  $\sim 70^\circ$ . The data are then stacked and combined into a movie that illustrates the tilt series in motion.

Each movie has  $\sim 100$  images collected with each image being  $\sim 1\text{--}3$  mB for total of  $\sim 100\text{--}300$  mB for each movie. The data is collected in a .tif format and the movies are rendered as .mp4.

### 2.2.1.3 Data Visualization and Analysis

Currently, Adobe Photoshop is being used to stitch data together to make gifs/movies of the automated tilt series. We will be developing in house algorithms to better align the datasets. In the future, programs like Avizo or Paraview will be used to model the data.

## 2.2.2 Transmission Electron Microscopy (TEM)

### 2.2.2.1 Overview

A GrandArm-300F STEM instrument is used to collect TEM and STEM images together with X-ray energy dispersive spectrometry (XEDS) elemental maps of samples. Figure 7 is presenting a 300 kV JEOL microscope that has the capability of high-resolution TEM and STEM imaging resulting atomic-scale imaging of the samples. Table 6 presents the data type for this microscope.



Figure 7. GranArm STEM in the Radiochemical Processing Laboratory at PNNL

Table 6. Description of the Data Volume, Associated Software Tools and Other Data for the GrandArm-300F STEM Equipment

Category	Value
Digital Platform Tag(s)	To be determined
Digital Point of Contact	Shalini Tripathi, Chinthaka Silva
Approximate Data Volume per Operation (GB)	5–20
Approximate Number of Operations per Year	~200
Associated Software Tools	DigitalMicrograph data processing software

#### 2.2.2.2 Data Collection and Transfer

TEM and STEM images and energy dispersive spectroscopy (EDS) elemental maps are usually saved in .tif format. The raw data is exported to an internal server and accessed remotely.

#### 2.2.2.3 Data Visualization and Analysis

DigitalMicrograph files are visualized using Gatan DigitalMicrograph software. All the analysis can be performed within that software.

## 2.2.3 Scanning Electron Microscopy (SEM)

### 2.2.3.1 Overview

Three different SEM have been used to this point. These are as follows:

- FEI Quanta FEG focused ion beam (FIB) presented in Figure 8. A data description is provided in Table 7. This instrument is capable of collecting SEM images, elemental maps using EDS, and prepare TEM specimens using FIB technique.
- Helios Hydra Plasma FIB. This microscope also capable of SEM imaging, EDS, and FIB lift-outs. This one also equipped with electron backscatter diffraction (EBSD) option.
- JEOL 7600 SEM. This SEM is specifically used for SEM and EBSD analysis of the samples.

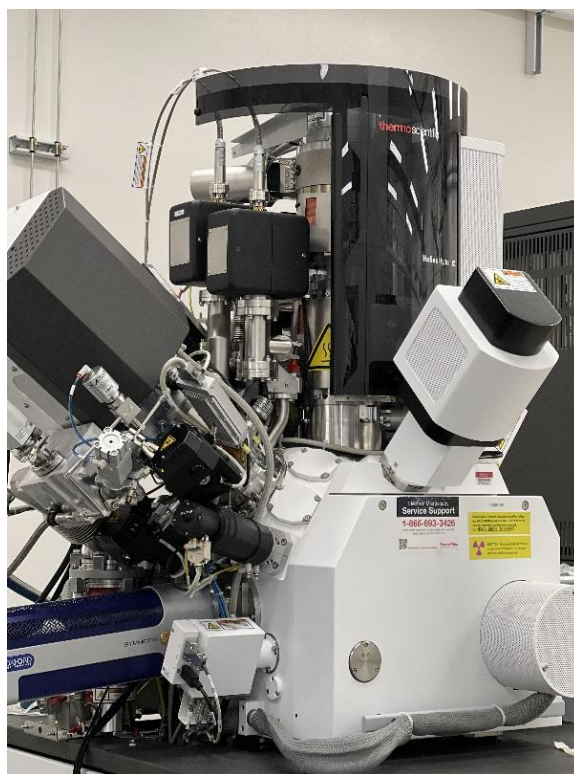


Figure 8. Helios Hydra Plasma FIB in the ESC Building

Table 7. Description of the Data Volume, Associated Software Tools and Other Data for the SEM Equipment

Category	Value
Digital Platform Tag(s)	To be determined
Digital Point of Contact	Tanvi Ajantiwalay, Chinthaka Silva
Approximate Data Volume per Operation (GB)	1–10
Approximate Number of Operations per Year	~300
Associated Software Tools	AZtec and AZtecCrystal data processing software

### 2.2.3.2 Data Collection and Transfer

SEM images and EDS elemental maps are usually saved in .tif format. EBSD scans are saved using instrument file formats (OIPX or H5OINA). Raw data are exported to an internal server and accessed remotely.

### 2.2.3.3 Data Visualization and Analysis

The OIPX format can be read using AZtec and H5OINA format using AZtecCrystal software. The analyzed data can be exported into .tif images that are used in preparing the final figures.

## 2.2.4 Microhardness Tester

### 2.2.4.1 Overview

A Microhardness Tester CM-802AT, Sun-Tec Corporation is used for hardness testing of the samples as presented in Figure 9. A general testing consists of an area containing 40 to 60 indents using 300 gf load with a 12-second duration. Table 8 provides the data description for this machine.



Figure 9. Microhardness Tester CM-802AT,<sup>1</sup> Sun-Tec Corporation in PNNL's 3410 Building

---

<sup>1</sup> <https://sunteccorp.com/equipment/micro-hardness-tester-cm-series-clark/>

Table 8. Description of the Data Volume, Associated Software Tools and Other Data for the Equipment D8 Discover

Category	Value
Digital Platform Tag(s)	To be determined
Digital Point of Contact	Angel Ortiz
Approximate Data Volume per Operation (GB)	~2 per file
Approximate Number of Operations per Year	~200
Associated Software Tools	OriginPro

#### 2.2.4.2 Data Collection and Transfer

Microhardness output data can be exported into an excel file. The data is shared using a server folder.

#### 2.2.4.3 Data Visualization and Analysis

Data visualization and analysis can be done in Microsoft Excel or in OriginPro software.

### 2.2.5 X-ray Diffractometer – D8 Discover by Bruker

#### 2.2.5.1 Overview

D8 Discover diffractometer is used to collect powder X-ray diffraction patterns of samples (Figure 10). This diffractometer is equipped with Cu K $\alpha$  radiation source and can operate at a maximum 1.6 W power (40 mA and 40 V). It has a large area-type detector allowing to scan a sample in a 10–105° 2 $\theta$  range in a less than 1 hour.



Figure 10. D8 Discover Powder X-Ray Diffractometer in the LSL2 Building

Table 9. Description of the Data Volume, Associated Software Tools and Other Data for the Equipment D8 Discover

Category	Value
Digital Platform Tag(s)	To be determined
Digital Point of Contact	Quin Miller
Approximate Data Volume per Operation (GB)	~2 MB per file
Approximate Number of Operations per Year	~200
Associated Software Tools	Bruker's EVA and HighScore Plus by Malvern Panalytical Ltd

### 2.2.5.2 Data Collection and Transfer

XRML or RAW files are the instrument generating files. Data can be exported into text formats. Data are usually sent by the operator in an email attachment.

### 2.2.5.3 Data Visualization and Analysis

The preferable data analysis software is HighScore Plus by Malvern Panalytical Ltd. The International Center for Diffraction Data database is also needed for the phase identification process. The General Structure Analysis System software is used to fit X-ray diffraction patterns using Rietveld analysis.

## 2.2.6 Sonix Fusion Acoustic Microscope

### 2.2.6.1 Overview

The Sonix Fusion Scanning Acoustic Microscope (Figure 11) is a highly versatile diagnostic tool for locating, classifying, and imaging internal defects and other microstructural features within a variety of items. A range of high frequency ultrasonic transducers and ultrasonic scanning methods can be used with the system.

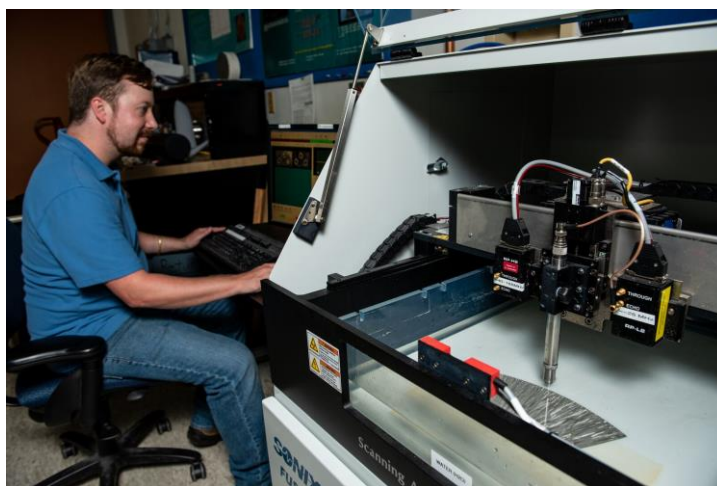


Figure 11. Sonix Fusion Scanning Acoustic Microscope

Table 10. Description of the Data Volume, Associated Software Tools and Other Data for the Sonix Fusion Scanning Acoustic Microscope

Category	Value
Digital Platform Tag(s)	To be determined
Digital Point of Contact	To be determined
Approximate Data Volume per Operation (GB)	0.500
Approximate Number of Operations per Year	100
Associated Software Tools	Vendor delivered, specialized Python scripts

### 2.2.6.2 Data Collection and Transfer

Wave forms in textual format.

### 2.2.6.3 Data Analysis and Visualization

Vendor delivered, specialized Python scripts.

## 2.2.7 Gas Pycnometer

### 2.2.7.1 Overview

Micromeritics, AccuPyc II 1340 (1, 5, 10 and 20 cm<sup>3</sup> measuring cells) gas pycnometer for powder particle density, density of solids and porosity measurements.



Figure 12. Micromeritics AccuPyc 1340 II

Table 11. Description of the data volume, associated software tools and other data for the Micromeritics AccuPyc 1340 II

Category	Value
Digital Platform Tag(s)	To be determined

Digital Point of Contact	Carolyn Burns
Approximate Data Volume per Operation (GB)	1-5 KB
Approximate Number of Operations per Year	~100
Associated Software Tools	To be determined

### 2.2.7.2 Data Collection and Transfer

Continued work needs for further development.

### 2.2.7.3 Data Visualization and Analysis

Continued work needs for further development.

## 2.2.8 Digital Microscope

### 2.2.8.1 Overview

Digital Microscope, Keyence VHX-7020, 4k Ultra-High Accuracy Microscope. Microscope capable of 20x -6000x magnification.



Figure 13. Keyence VHX-7020 Digital Microscope

Table 12. Description of the data volume, associated software tools and other data for the Keyence VHX 7020 Digital Microscope

Category	Value
Digital Platform Tag(s)	To be determined
Digital Point of Contact	Joshua Silverstein
Approximate Data Volume per Operation (GB)	10-66MB
Approximate Number of Operations per Year	~500
Associated Software Tools	Keyence image analysis software

### 2.2.8.2 Data Collection and Transfer

Images can be saved in TIFF format. The raw data can be stored on the hard drive or transferred to a server.

### 2.2.8.3 Data Visualization and Analysis

Digital images can be visualized by vendor provided software.

## 2.3 Heat Treatment Equipment

### 2.3.1 Furnaces

#### 2.3.1.1 Overview

Furnace CM H<sub>2</sub> Furnace Model 1516GSH2FL used to sinter 3D printed parts. Maximum temperature 1450 °C, fully programable for hold, ramp, and step protocols.



Figure 14. Furnace CM H<sub>2</sub> Furnace Model 1516GSH2FL

Table 13. Description of the data volume, associated software tools and other data for the CM H<sub>2</sub> Furnace

Category	Value
Digital Platform Tag(s)	To be determined
Digital Point of Contact	Lorraine Seymour
Approximate Data Volume per Operation (GB)	To be determined
Approximate Number of Operations per Year	~50
Associated Software Tools	To be determined

### 2.3.1.2 Data Collection and Transfer

Continued work needs for further development.

### 2.3.1.3 Data Visualization and Analysis

Continued work needs for further development.

## 2.4 Materials Modeling Tool

### 2.4.1 ANSYS LS-DYNA Software

#### 2.4.1.1 Overview

LS-DYNA is an advanced general-purpose multiphysics simulation software package developed by the Livermore Software Technology Corporation, which was acquired by Ansys in 2019. LS-DYNA's core-competency lie in highly nonlinear transient dynamic simulation using explicit time integration. The meshfree Lagrangian-based Smoothed Particle Hydrodynamics (SPH) method available in LS-DYNA can be used to model thermomechanical processes with extremely large material deformation and complicated tool/material contacts. The list of the properties that can be calculated with SPH in LS-DYNA software is shown below, and Table 14 shows the typical data volume and associated software tools for this method:

- Material kinetic status: locations, velocities, and accelerations
- Material physical properties: stress-strain states, temperature, forces, moments
- Material micro/mesoscale properties: dislocation densities, grain sizes
- Contact responses: friction, forces, energy generation
- Thermomechanical material behaviors: more than 200+ material constitutive models.

Table 14. Description of Data Volume and Associated Software Tools for the SPH in LS-DYNA Software

Category	Value
Associated Software	Pre- and post-processing the SPH model (does not require significant storage)

Category	Value
Tools: LS-PrePost	space)
LS-Run	Program to run SPH model and manage existing runs (does not require significant storage space)
Data generated	50–100 GB (require significant storage space)

#### 2.4.1.2 Data Collection and Transfer

All the basic data from SPH modeling results are generated and stored in d3plot file format. Additional data from SPH results can be requested and stored in binout file, either in binary format or in ASCII format. The d3plot and binout files can be opened by LS-PrePost to generate movie (format live .avi, .mov, .mp4), picture (format like .jpeg, .tif, .png), and raw (crv, xlsx, xy pair) data. Transferring d3plot and binout file may require significant storage space and read/writing speed because their file sizes are large. Transferring post-process data such as movie, picture, and raw data are inexpensive and do not have special requirements.

#### 2.4.1.3 Data Visualization and Analysis

LS-PrePost is needed to open the d3plot and binout files to visualize the modeling result. The data can be extracted from d3plot and binout files and analyzed using LS-PrePost. The visualization data can be exported to movies (.avi, .mov, .mp4), picture (.jpeg, .tif, .png), and raw data (.crv, .xlsx, .xy pair). Movie and picture data can be used directly. The raw data can be accessed by Matlab or Microsoft Excel for data processing and plot generation.

### 2.4.2 Thermo-Calc 2000b Software

#### 2.4.2.1 Overview

Thermo-Calc and the Add-on Modules can be used to calculate a broad range of materials properties for multicomponent systems as a function of temperature and composition when used in conjunction with suitable databases. The list of the properties that can be calculated with Thermo-Calc software is shown below, and Table 15 shows the typical data volume:

- Phase equilibria
- Physical properties
- Kinetic coefficients
- Mechanical properties
- Non-equilibrium Solidification Properties
- Steel Model Library (kinetics)
- Nickel Model Library (kinetics)
- Process Metallurgy (slag chemistries, etc.)
- Diffusion Module (Micro segregation, Homogenization, precipitate coarsening, etc.)

Table 15. Description of Data Volume and Associated Software Tools for the Thermo-Calc 2020b Software

Category	Value
Associated Software Tools: TCHEA3 database	Linked to the Thermo-Calc Software (does not require significant storage space)
Data generated	Kilo-Mega Bytes (does not require significant storage space)

#### 2.4.2.2 Data Collection and Transfer

The data such as phase diagrams or phase fraction versus temperature plots are generated in a picture format such as .tif, .png, or .jpeg.

#### 2.4.2.3 Data Visualization and Analysis

No special software is needed to visualize and analyze the generated data. The data generated can also be exported to .tif or .png formats which can be accessed using stock Microsoft Photos Application.

## 3.0 Experimental Equipment and Simulation Tools: INL

### 3.1 Mechanical Testing and Characterization Equipment

#### 3.1.1 ZEISS XRadia 520 Versa

##### 3.1.1.1 Overview

The ZEISS Xradia 520 Versa X-ray microscope volumetrically images samples nondestructively using X-ray computed tomography (Figure 15). The Versa uses a tungsten target to produce an X-ray spectrum, with maximum energy ranging from 30 kVp to 160 kVp and a maximum power of 10 W. This instrument has two imaging capabilities. The first is its flat panel detector that provides a field-of-view (FOV) of 30.7 cm × 19.4 cm and spatial resolutions ranging from 100 µm/pixel to 6 µm/pixel. The other imaging modality is the microscope which consists of four objective lenses, has a FOV of 0.6 mm × 0.6 mm with spatial resolution ranging from 55 µm/pixel to ~0.2 µm/pixel.



Figure 15. ZEISS Xradia 520 Versa X-ray Microscope.

Table 16. Description of the Data Volume, Associated Software Tools and Other Data for the ZEISS Xradia 520 Versa X-ray Microscope Used at INL.

Category	Value
Digital Platform Tag(s)	X-ray CT, Zeiss Xradia 520 Versa X-ray Microscope
Digital Point of Contact	William Chuirazzi
Approximate Data Volume per Operation (GB)	5–50
Approximate Number of Operations per Year	300
Associated Software Tools	ZEISS reconstruction software, Dragonfly, AVIZO

##### 3.1.1.2 Data Collection and Transfer

Once a CT scan is completed, the radiographs (a .txrm file) and reconstructed slices (a .txm file) is transferred to an encrypted hard drive where it is then transferred to networked computers. Data are stored on a shared networked drive that users of the Versa have access to. Copies of this data are also transferred to other networked drives that customers can access. Basic metadata (spatial resolution, detector dimensions, image acquisition time, etc.) is stored as a .txt file with additional information (detector, stage and source positions) stored as .png or .jpeg screenshots, as needed.

### 3.1.1.3 Imaging

The ZEISS Xradia 520 Versa can range from FOVs from 30.7 cm × 19.4 cm down to 0.6 mm × 0.6 mm with spatial resolution varying from 100 μm/pixel down to ~0.2 μm/pixel, depending on the sample size, geometry, and composition. This machine is primarily used for nondestructive three-dimensional (3-D) imaging to quantify cracks, porosity, interfaces between different layers or materials, and geometric changes. This information is useful for 1) modeling efforts and 2) to inform targeted destructive analysis. This technique also has the capability to perform X-ray radiography and tomography of samples under compression and tensile testing, as well as other imaging modalities such as diffraction contrast tomography, which can show the grains of a material and their 3-D alignment.

### 3.1.1.4 Data visualization and Analysis

After the radiographs are acquired, the ZEISS Scout-and-Scan software is usually used for image reconstruction to produce the 3-D dataset. However, custom reconstruction packages such as TIGRE or ASTRA can also be used to reconstruct nonstandard samples. These reconstruction packages are accessed using either Python or MATLAB. Once the reconstructions are complete, image segmentation and quantified data extraction are performed with either MATLAB or a commercial software such as Object Research Systems (ORS) Dragonfly or ThermoFisher Avizo. Dragonfly and Avizo are also used to create 3-D renderings of data, such as figures for publications and/or presentations.

## 3.1.2 Servo-hydraulic load frames

### 3.1.2.1 Overview

INL typically employs MTS Systems servo-hydraulic load frames for cyclic testing, including fatigue and creep fatigue testing (Figure 16). Servo-hydraulic machines test samples with force as a function of time generated by hydraulic systems and measure displacements using electronic control and measurement systems. Section 2.2 will provide a summary of the information for the machines that is generally relevant, and specific machine data will be provided upon contribution of individual datasets.

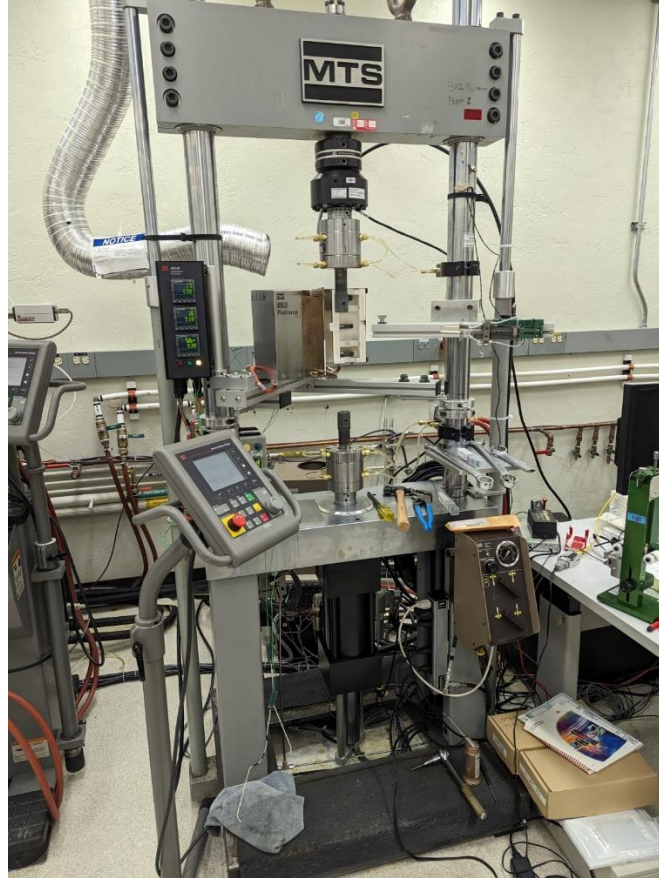


Figure 16. Typical MTS Servo-Hydraulic Load Frame at INL

Table 17. Description of the Data Volume, Associated Software Tools and Other Data for a Generic MTS Servo-Hydraulic Machine at INL

Category	Value
Digital Platform Tag(s)	Machine name, test type
Digital Point of Contact	Michael McMurtrey
Approximate Data Volume per Operation (GB)	~0.001--~0.5
Approximate Number of Operations per Year	10-100

### 3.1.2.2 Data Collection and Transfer

MTS Testsuite software is used to control the frames and collect data. Important information includes specimen metadata (typically key geometry measurement, material, and specimen identification [ID]). During the actual test, two sets of data are collected, time stamped data at set intervals, and peak/valley strain and stress, which records a single value for each cycle (the maximum and minimum values of the strain/stress for that cycle). Along with time stamped data, notes are also sometimes recorded to data files to include information about power outages, restarts, or other oddities.

Table 18. Typical Data Collected In Tests on the Servo-Hydraulic Machines at INL

Information	Data categories	File type	Size
Sample metadata	Gauge diameter, gauge length, material type, sample ID	.txt/.CSV	Negligible
Results time series	Time stamp, cycle number, temperature (typically two values), displacement, force, strain (calculated), stress (calculated), peak/valley stress (one value per cycle), peak/valley strain (one value per cycle), notes	.CSV/Excel	~1 to 100s MB, depending on test type and test duration

### 3.1.2.3 Data Visualization and Analysis

Data are generally analyzed using typical office software (e.g., Microsoft Excel, Microsoft Word) and/or coding libraries for data analysis (e.g., Python). No special software is required.

## 3.1.3 Electro-mechanical Load Frames

### 3.1.3.1 Overview

INL typically employs electro-mechanical load frames (e.g., Instron machines) for tensile testing. Electro-mechanical load frames are essentially functionally equivalent to servo-hydraulic load frames, differing only by the mechanism by which the force is generated (Figure 17). Electromechanical load frames use a screw driven by an electrical motor to generate motion.



Figure 17. Typical Electro-Mechanical Load Frame at INL

Table 19. Description of the Data Volume, Associated Software Tools and Other Data for a Generic Electro-Mechanical Load Frame at INL

Category	Value
Digital Platform Tag(s)	Machine name, test type
Digital Point of Contact	Michael McMurtrey
Approximate Data Volume per Operation (GB)	~0.001—~0.01
Approximate Number of Operations per Year	10-1,000

### 3.1.3.2 Data Collection and Transfer

Bluehill 2, Bluehill 3, Bluehill Universal, and Console are softwares used to control frames and collect data. Similar data are collected as with the servo-hydraulic test frames; however, tensile tests are relatively short, and so data files tend to be much smaller.

Table 20. Typical Data Collected in Tests on the Electro-Mechanical Load Frames at INL

Information	Data categories	File type	Size
Sample metadata	Gauge diameter, gauge length, material type, sample ID	.txt/.CSV	Negligible
Results time series	Time stamp, cycle number, temperature (typically two values), displacement, force, strain (calculated), stress (calculated), notes	.CSV/Excel	~1 to 10 MB

### 3.1.3.3 Data visualization and analysis

Data generally are analyzed using typical office software (e.g., Microsoft Excel, Microsoft Word) and/or coding libraries for data analysis (e.g., Python). No special software is required.

## 3.1.4 Static Load Frames

### 3.1.4.1 Overview

INL uses Applied Test Systems static load frames for creep testing that are either direct loaded or loaded over a lever arm to multiply the weight (20:1 or 3:1) (Figure 18).



Figure 18. Typical Static Load Frame at INL

Table 21. Description of The Data Volume, Associated Software Tools and Other Data for a Static Load Frame at INL

Category	Value
Digital Platform Tag(s)	Machine name, test type
Digital Point of Contact	Michael McMurtrey
Approximate Data Volume per Operation (GB)	~0.001--~0.01
Approximate Number of Operations per Year	~10

#### 3.1.4.2 Data Collection and Transfer

The WinCCS program is used to control the Applied Test Systems frames and collect data. While these tests are the longest running mechanical tests, as changes are slow to occur, data is not collected at a rapid pace, resulting in relatively small data files compared to cyclic testing.

Table 22. Typical Data Collected in Tests on the Static Load Frames at INL

Information	Data categories	File type	Size
Sample metadata	Gauge diameter, gauge length, material type, sample ID	.txt/.CSV	Negligible
Results time series	Time stamp, temperature (typically three values), displacement (typically two values), average strain (calculated), notes	.CSV/Excel	~10 MB

### 3.1.4.3 Data visualization and analysis

Data are generally analyzed using typical office software (e.g., Microsoft Excel, Microsoft Word) and/or coding libraries for data analysis (e.g., Python). No special software is required.

## 3.1.5 Hardness Testing

### 3.1.5.1 Overview

INL uses both Rockwell and Vickers hardness indenters for measurement of material hardness (Figure 19). A Rockwell tester uses a spherical ball as the indenter tip, while a Vickers tester uses a pyramidal diamond as the indenter tip.



Figure 19. Rockwell Hardness Indenter (left) and Vickers Indenter (right) at INL

Table 23. Description of the Data Volume, Associated Software Tools and Other Data for Generic Hardness Testing at INL

Category	Value
Digital Platform Tag(s)	Machine name, test type
Digital Point of Contact	Michael McMurtrey
Approximate Data Volume per Operation (GB)	<0.001
Approximate Number of Operations per Year	~100–1,000

### 3.1.5.2 Data Collection and Transfer

While a single value is typically reported, this usually is the average of multiple measurements (30 measurements is typical) that make up the raw data to be stored. This does not represent a significant challenge for data storage given the small file sizes and limited data that needs to be recorded.

Table 24. Typical Data Collected During Hardness Testing at INL

Information	Data categories	File type	Size
Sample metadata	Material type, sample ID, machine type	.txt/.CSV	Negligible
Results	Hardness measurements, notes	.CSV/Excel	Negligible

### 3.1.5.3 Data Visualization and Analysis

Data are generally analyzed using typical office software (e.g., Microsoft Excel, Microsoft Word) and/or coding libraries for data analysis (e.g., Python). No special software is required.

## 3.1.6 Optical Microscopes

### 3.1.6.1 Overview

INL has several optical microscopes that can be used for optical metallography, as well as topographical measurements (Figure 20). Optical metallography may be used to look for relatively large defects, or grain structure (typically etched specimens). This results in a two-dimensional image file. Topographical measurements are typically used to examine roughness or examine aspects of fracture surfaces.

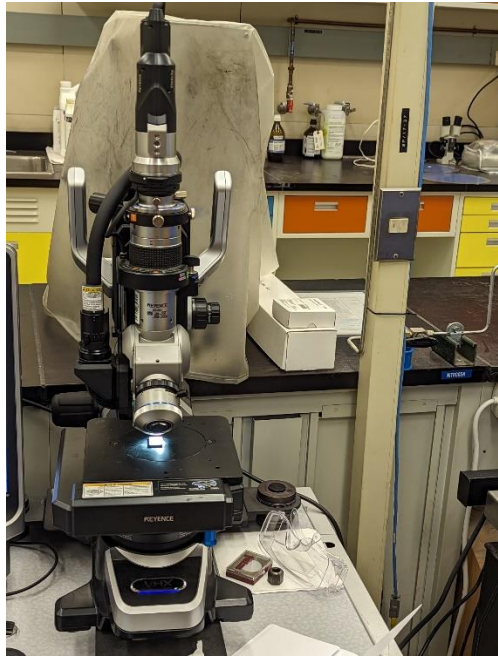


Figure 20. Typical Optical Microscope at INL

Table 25. Description of the Data Volume, Associated Software Tools and Other Data for a Generic Optical Microscope at INL

Category	Value
Digital Platform Tag(s)	Machine name, test type
Digital Point of Contact	Michael McMurtrey
Approximate Data Volume per Operation (GB)	<0.001
Approximate Number of Operations per Year	~100–1,000

### 3.1.6.2 Data Collection and Transfer

Data are collected via digital image sensor and processed by microscope-specific software. Specific details will be provided for each data series.

Table 26. Typical Data Collected in Optical Microscopy Examination at INL

Information	Data categories	File type	Size
Sample metadata	Material type, sample ID, microscope name, software version	.txt/.CSV	Negligible
Results	Image, potentially with height values associated with	.tiff file .jpg/.tiff	~1–20 MB

### 3.1.6.3 Data Visualization and Analysis

Data are generally analyzed using typical office software (e.g., Microsoft Excel, Microsoft Word) and/or coding libraries for data analysis (e.g., Python). No special software is required.

### 3.1.7 Electron Microscopes

#### 3.1.7.1 Overview

INL has access to both SEM and TEM electron microscopes (Figure 21). TEM is typically used for very high-resolution images, such as examination of fine ( $<1\ \mu\text{m}$ ) precipitate structures or dislocations. SEM is used for lower resolution examination, such as broad views of grain structure. Both techniques can be used for standard imaging to produce a two-dimensional image file but can also be used for compositional studies (e.g., EDS) or diffraction studies (e.g., EBSD), which result in larger data files. For both cases, the two-dimensional image contains more than just a grey scale value. It also contains values for the elemental compositions (percentages of each element with spatial information) or phases and orientation maps (spatially stored data, potentially with diffraction patterns as well, though that is less commonly saved as it creates gigabytes of data).



Figure 21. Quanta FEG 650 SEM at INL

Table 27. Description of the Data Volume, Associated Software Tools and Other Data for a Generic Electron Microscope at INL

Category	Value
Digital Platform Tag(s)	Machine name, test type
Digital Point of Contact	Michael McMurtrey
Approximate Data Volume per Operation (GB)	0.1–10
Approximate Number of Operations per Year	~100–1,000

#### 3.1.7.2 Data Collection and Transfer

Data are collected via digital image sensor and processed by microscope-specific software. Specific details will be provided for each data series.

Table 28. Typical Data Collected in Electron Microscopy Examinations at INL

Information	Data categories	File type	Size
Sample metadata	Material type, sample ID, microscope name, software version	.txt/.CSV	Negligible
Results	Image, potentially with compositional values and/or phases and orientations associated with .tiff file	.jpg/.tiff	~10s–100s MB

### 3.1.7.3 Data Visualization and Analysis

Data are generally visualized and initially analyzed using specific software (to be specified for each data series). Typical office software (e.g., Microsoft Excel, Microsoft Word) and/or coding libraries for data analysis (e.g., Python) may also be required for further analysis after data extraction from the raw file.

## 3.1.8 Neutron Irradiation Testing

### 3.1.8.1 Overview

Neutron irradiations at INL can be performed in several reactors, including the Advanced Test Reactor (ATR), the Transient Reactor Test facility, and the Neutron Radiography reactor. Neutron irradiations for the AMMT program will most likely involve irradiation at ATR, and this section will focus on describing that, with additional reports generated as necessary if other neutron reactor irradiations occur.

Neutron irradiation campaigns generate significant pre-irradiation and post-irradiation analysis data. The analysis data is collected into the Engineering Calculations and Analysis (ECAR) document. The ECAR document is an extensive collection of all the engineering analysis performed for the irradiation campaign and includes details of the Monte Carlo N-Particle (MCNP) and the ORIGEN2 simulations of full-core neutronics calculations. The pre-irradiation analysis computes the predicted behavior during the expected power history, while the post-irradiation analysis computes the as-run behavior using the actual power history during the irradiation. The purpose of the analysis is to calculate heat generation rates of test specimens and components, the radiation damage (dpa) for each capsule, and decay heat and source terms (isotopic composition and radioactive decay) as a function of time after sample removal from the reactor. The ECAR document also contains the information regarding the specimen holder specification (e.g., material, geometry, fill gas, etc.), the irradiation location in the reactor, and the cycle numbers of the irradiations.

In addition, finite element method (FEM) analysis in three dimensions can be performed to visualize the temperature distribution and damage distribution of the specimens.

Table 29. Description of the Data Volume, Associated Software Tools and Other Data for a Neutron Irradiation Campaign at INL

Category	Value
Digital Platform Tag(s)	Reactor name, analysis type
Digital Point of Contact	Drew Johnson
Approximate Data Volume per Operation (GB)	0.1–10

### 3.1.8.2 Data Collection and Transfer

The ECAR document is a portable document file (pdf) with a file size on the order of megabytes. It should be transferred from the engineering analysis team to the irradiation lead for upload into the MDDC. The ECAR document contains link addresses to the data files on INL servers used to generate the engineering analysis, as well as raw data output from the analysis and the ATR power history by cycle for the relevant cycles. If the ORIGEN2, MCNP and specimen geometry engineering drawing are deemed necessary to collect in the future, an update to the MDDC entry for neutron irradiations should be processed.

The finite element analysis is typically performed with the Abaqus software, the specific details of which should be provided to the MDDC for each analysis.

**Table 30. Typical Data Collected for Neutron Irradiations at INL that may not be within the ECAR Document**

Information	Data Categories	File Type	Size
Irradiation Metadata	Sample ID	.Txt/.CSV	Negligible
FEM Results	Input Mesh Files, Input Run Files, Output Mesh Files	.Inp/.Odb (Typical Abaqus Formats)	~0.001–10

### 3.1.8.3 Data Visualization and Analysis

The FEM results must be viewed with an FEM viewer (if performed with Abaqus, they can be viewed within the Abaqus software). The ECAR document can be viewed with a pdf viewer.

## 3.2 Heat Treatment Equipment

### 3.2.1 Furnaces

#### 3.2.1.1 Overview

INL has various box, clamshell, and tube furnaces used for statically heating material (no applied stress) (Figure 22). These are used to solution anneal or heat treat a material, or to study the effects of long-term aging.



Figure 22. Typical Box Furnace Set-Up at INL

Table 31. Description of the Data Volume, Associated Software Tools and Other Data for Furnace Testing at INL

Category	Value
Digital Platform Tag(s)	Machine name, test type
Digital Point of Contact	Michael McMurtrey
Approximate Data Volume per Operation (GB)	<0.001
Approximate Number of Operations per Year	~100–1,000

### 3.2.1.2 Data Collection and Transfer

Time versus temperature is typically the main data recorded, and the files are not generally very large, even for long term aging. Data are collected automatically from direct sensor outputs.

Table 32. Typical Data Collected in Furnace Tests at INL

Information	Data categories	File type	Size
Sample metadata	Material type, sample ID, furnace type, atmosphere composition	.txt/.CSV	Negligible
Results time series	Temperature, notes	.CSV/Excel	~1 MB

### 3.2.1.3 Data Visualization and Analysis

Data are generally analyzed using typical office software (e.g., Microsoft Excel, Microsoft Word) and/or coding libraries for data analysis (e.g., Python). No special software is required.

### 3.3 Materials Modeling Tool

#### 3.3.1 LAMMPS

##### 3.3.1.1 Overview

Large-scale Atomic/Molecular Massively Parallel Simulator (LAMMPS) is a free and open-source molecular dynamics program maintained by Sandia National Laboratories and available at <https://lammps.org> (Figure 23). LAMMPS is designed to efficiently run large molecular dynamics (MD) simulations by using Message Passing Interface (MPI) to spatially discretize a simulation into subdomains that are distributed across the available high-performance computing (HPC) resources.

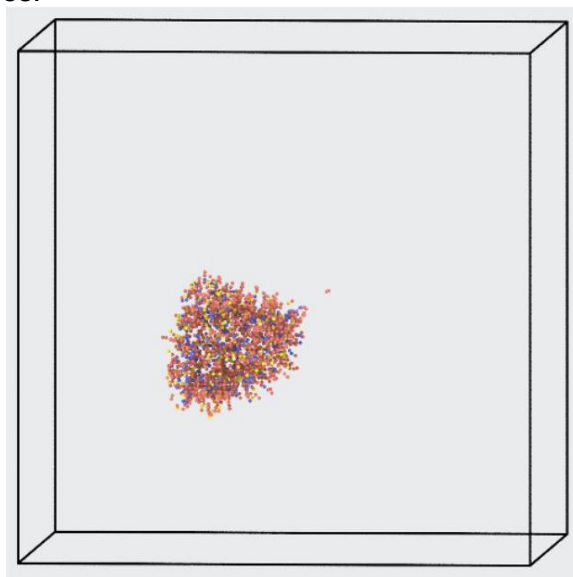


Figure 23. Early Stage of a Collision Cascade in Fe-Cr-Ni (red, blue, and yellow, respectively) Simulated by Molecular Dynamics Using LAMMPS and Visualized Using OVITO

Table 33. Description of the Data Volume, Associated Software Tools, and Other Data for LAMMPS Use at INL

Category	Value
Digital Platform Tag(s)	LAMMPS
Digital Point of Contact	Andrea Jokisaari
Approximate Data Volume per Operation (GB)	3 per simulation
Approximate Number of Operations per Year	1,000
Associated Software Tools	OVITO

##### 3.3.1.2 Data Generation

LAMMPS is installed on the HPC system being used to run the calculations. The simulation methodology is detailed in a text file known as a LAMMPS input script that contains a list of commands instructing the software on how to construct the initial configuration of atoms, which boundary conditions to apply, how the atoms will interact with each other, and what

measurements to collect. There are currently a several different input script templates used to study different phenomena (collision cascades, point defect diffusion measurements, etc.).

**Table 34. Description of the high-performance computing needs for LAMMPS use at INL.**

<b>System Requirements</b>	<b>Value</b>
Compilation Requirements	CMake, Fortran (gfortran), C (gcc), C++ (g++), MPI (OpenMPI), FFTW, BLAS, CUDA (if running on gpu) Memory: <4 GB Disk: 4 GB
Operating System	Linux (POSIX)
Code Versioning System	Continuous stable branch

### 3.3.1.3 Data Collection and Transfer

In general, LAMMPS simulations output two main forms of data: thermodynamic data and atom configuration data. Thermodynamic data are saved to the hard drive as a text file containing a table of the thermodynamic variables. The text file begins with a header line containing each variable name being output. The remainder of the file is a table with the value of each variable being calculated separated by spaces, with each new line corresponding to a different timestep in the simulation. Files containing thermodynamic output from LAMMPS will typically use 25 MB of hard drive space.

The second form of output is a LAMMPS trajectory file that is saved to the hard drive and contains snapshots of the atom configuration at various points during the simulation as set in the input file. The trajectory file is a text file that starts with the initial snapshot of the starting configuration to which additional snapshots are appended to the end of the file. Each snapshot starts with a header detailing the timestep of the snapshot, the number of atoms in the simulation, the dimensions of the simulation box, and the names of the per-atom variables being output (atom id, atom species, and position coordinates). This is then followed by the per-atom data for each atom in the system on a new line. Trajectory files contain a lot of information and can be very useful when analyzing the results of the molecular dynamics simulation. However, the files also consume a large amount of hard drive space. One of these files will typically use around 300 MB of hard drive space per snapshot stored in the file.

These output files are normally downloaded to a user's workstation for further analysis.

### 3.3.1.4 Data Visualization and Analysis

LAMMPS trajectory files can be visualized using the OVITO software package. OVITO can display a timeline of the atom configurations and analyze the structure of the atoms in the simulation. There are several analysis methods that are particularly useful. The first method is Wigner-Seitz, which can identify either vacancies or interstitials in the lattice structure. Another useful method is Dislocation Analysis, which can locate defects in a lattice structure and identify defect loops in the configuration of atoms.

### 3.3.1.5 Metadata

Table 35. Metadata Table for LAMMPS Software Use at INL

Field name	Metadata Information	DB Table	DB Key
LAMMPS Version	Version of LAMMPS for compatibility reasons	sim_info	version_id
Simulation Name	Descriptive simulation name, indicating what is being measured	sim_info	sim_name
Potential Energy Model	Name of potential energy model	sim_info	PE_model
HPC input script	HPC input script detailing the hardware used to run the calculation, how many MPI nodes and OMP threads were used	sim_info	Hardware_info
Atom Configuration	Initial crystal structure and lattice constants	sim_info	Init_crystal
Material Composition	List of atom species and the atom percent composition	sim_info	composition

### 3.3.2 Vienna Ab Initio Simulation Package (VASP)

#### 3.3.2.1 Overview

The VASP software applies density functional theory to accurately account for quantum effects and provides information that can be used by larger length-scale methods, such as molecular dynamics, kinetic Monte Carlo, and phase field modeling (Figure 24). VASP can be found at <https://www.vasp.at/>. VASP leverages MPI to efficiently run on HPC systems.

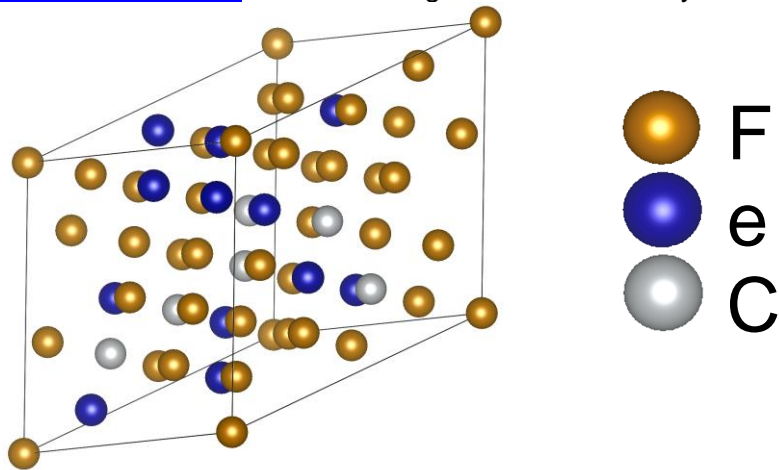


Figure 24. Representation of an Fe-Cr-Ni System Calculated by VASP and Visualized with VESTA

Table 36. Description of the Data Volume, Associated Software Tools and Other Data for VASP Use at INL

Category	Value
Digital Platform Tag(s)	VASP

Digital Point of Contact	Andrea Jokisaari
Approximate Data Volume per Operation (GB)	5–50, depending on simulation details
Approximate Number of Operations per Year	100+
Associated Software Tools	MPI, Python, matplotlib, Microsoft Excel, VESTA

### 3.3.2.2 Data Generation

A minimum of four text-based input files are required to run a VASP calculation: 1) a POSCAR file (describing the position of the atoms), 2) a POTCAR file (describing pseudopotential information for each element, which facilitates calculation of electronic energy near the nucleus), 3) an INCAR file (which defines the various options for the simulation), and 4) a KPOINTS file (which determines the coarseness of the reciprocal space grid). A VASP executable binary file is also required, several of which are available on the INL HPC storage system. These executable files include those that allow for calculation of energy barriers and that account for the unaligned electronic spin found in SS-316 at operating temperatures.

Table 37. Description of the High-Performance Computing Needs for VASP Use at INL

System Requirements	Value
Compilation Requirements	Fortran, C, C++ (i.e., GCC 10+ or NVIDIA HPC-SDK); FFTW, BLAS, LAPACK, and ScaLAPACK (i.e., intel-oneapi-mkl); MPI (i.e., intel-oneapi-mkl) Memory: 32 GB+ Disk: 100 GB+
Operating System	Linux (POSIX)
Code Versioning System	Continuous stable branch

### 3.3.2.3 Data Collection and Transfer

VASP calculations produce data largely in text-based files with the largest files being in binary files, with sizes ranging from 5 kB–3 GB. The file sizes depend on simulation parameters, such as how fine the k-point mesh is in the KPOINTS file and how high the ENCUT value is in the INCAR. These files are stored in the same folder in which the simulation is run and can be transferred between computer systems by standard file transfer tools (i.e., rsync and scp).

### 3.3.2.4 Metadata

Information on the simulation environment will be collected for each individual VASP simulation, including the code version, the k-point mesh, settings in the INCAR file, and converged ionic positions. This metadata will aid in connecting the VASP settings and inputs that run the simulation to the individual simulation results and generated data.

### 3.3.2.5 Data Visualization and Analysis

Analysis and postprocessing of the generated simulation data are expedited by using commonly available software. Generally, all data files are parsed and analyzed in the form of line and scatter plots. These data may be processed with software such as Python or Microsoft Excel. The Visualization for Electronic and Structural Analysis software is used to analyze and image crystal structures.

### 3.3.3 Multiphysics Object-Oriented Simulation Environment (MOOSE)

#### 3.3.3.1 Overview

The MOOSE software is used to conduct multiscale, multiphysics simulations in a wide range of fields, including that of microstructure- and environment-sensitive mechanical response of materials (Figure 25). Both finite element method and finite volume method implementations are available in MOOSE, and documentation of the framework can be found at <https://mooseframework.inl.gov/>. Primarily, the FEM approach is used for mechanical performance and microstructure evolution simulations. Finite volume approach is used for fluid dynamics models and are currently being explored in conjunction with the process modeling for additive manufacturing. An open-source, continuously developed software, MOOSE is available for download from <https://github.com/idaholab/moose>. The MOOSE software also forms the basis for the MALAMUTE and MARMOT codes, used for simulating advanced manufacturing processes, including their influence of materials, and microstructure evolution in nuclear environment, respectively.



Figure 25. Logo of the MOOSE Framework from INL

Table 38. Description of the Data Volume, Associated Software Tools and Other Information for MOOSE Use at INL

Category	Value
Digital Platform Tag(s)	MOOSE software, git commit hash available
Digital Point of Contact	Cody Permann, Andrea Jokisaari
Approximate Data Volume per Operation (GB)	1–500, depending on simulation details
Approximate Number of Operations per Year	1,000+
Associated Software Tools	MALAMUTE, MARMOT, MPI, PETSc, libMesh, Paraview, Python, VSCode, matplotlib, CUBIT, Microsoft Excel

#### 3.3.3.2 Data Generation

At least three files are required to run a MOOSE simulation: 1) a MOOSE executable binary file, 2) a text-based input file, and 3) an Exodus-based mesh file.

Prebuilt executable binaries for the MOOSE software are not available for most computer systems. After the source code is downloaded from the github repository, the executable binary must be compiled as detailed in the documentation available in [https://mooseframework.inl.gov/getting\\_started/installation/index.html](https://mooseframework.inl.gov/getting_started/installation/index.html). The minimum computer system requirements to build a MOOSE executable and run a MOOSE simulation are given

below. The INL HPC software does provide prebuilt executable binaries that are compiled monthly for users with access to the HPC system.

A text-based input file, formatted according to the MOOSE Language standards, is used to specify the field variables, governing and constitutive equations, output data types, and solver settings relevant to the physics of interest for the simulation. A text file editor is required to write the input files; the editor VSCode, with the MOOSE Language Support extension, is recommended. Additional input information may be required in the form of the supplemental CSV files, depending on the specific simulation needs. These supplemental files must be declared in the input file.

Generally, an external dedicated mesh generating software (i.e., CUBIT or gmsh) is used to produce an Exodus mesh file. Meshes constructed of Quad (two-dimensional) or Hex (3-D) FEM elements are recommended. In simple geometry cases, the internal MOOSE mesh generator may be used, through the input file, to create the mesh file.

**Table 39. Description of the High-Performance Computing Needs for MOOSE Use at INL**

System Requirements	Value
Compilation Requirements	C++17 compiler (GCC or Clang) Memory: 16 GB+ Disk: 30 GB+
Operating System	Mac OS 10.13+, Linux (POSIX)
Code Versioning System	Continuous stable branch, git

### 3.3.3.3 Data Collection and Transfer

The data generated by MOOSE by the MOOSE simulation may include CSV files, anticipated size 5 kB–1 GB, Exodus and Nemesis files, anticipated size 1–500 GB, and JSON files, anticipated size 5 kB–1 GB (Figure 26). The generated data file sizes will depend on the unique simulation details and on the level of resolution selected by the user. These data files will be created on the same computer system in which MOOSE simulation is run. The data files can be transferred between computer systems using standard file transfer tools, such as rsync and scp.

### 3.3.3.4 Metadata

```

Framework Information:
MOOSE-Version:.....git-commit-430828dbe1-on-2023-06-15
LibMesh-Version:.....
PETSc-Version:.....3.16.6
SLEPc-Version:.....3.16.2
Current-Time:.....Fri-Jun-23-09:32:56-2023
Executable-Timestamp:....Wed-Jun-21-13:29:50-2023

Parallelism:
--Num-Processors:.....2
--Num-Threads:.....1

Mesh:
--Parallel-Type:.....replicated
--Mesh-Dimension:.....3
--Spatial-Dimension:.....3
--Nodes:.....
--Total:.....4913
--Local:.....2631
--Min/Max/Avg:.....2282/2631/2456
--Elems:.....
--Total:.....512
--Local:.....256
--Min/Max/Avg:.....256/256/256
--Num-Subdomains:.....1
--Num-Partitions:.....2
--Partitioner:.....metis

Nonlinear System:
--Num-DOFs:.....14739
--Num-Local-DOFs:.....7893
--Variables:.....{"disp_x","disp_y","disp_z"}
--Finite-Element-Types:...."LAGRANGE"
--Approximation-Orders:...."SECOND"

Execution Information:
--Executioner:.....Transient
--TimeStepper:.....ConstantDT
--TimeIntegrator:.....ImplicitEuler
--Solver-Mode:.....Preconditioned-JFNK
--MOOSE-Preconditioner:....SMP

```

Figure 26. Metadata from a MOOSE Simulation, Demonstrating the Type of Information to be Collected with a Mechanics Simulation Example

Information on the simulation environment will be collected for each individual MOOSE simulation, including the code revision information (through the git commit hash), the mesh characteristics, the nonlinear field variable, and the simulation solver settings. This metadata will aid in connecting the state of the MOOSE code, used to build the executable file, to the individual simulation results and generated data.

### 3.3.3.5 Data Visualization and Analysis

Analysis and postprocessing of the generated simulation data is expedited by using commonly available software. Analysis procedures and approaches differ, depending on the simulation details.

Generated data stored in CSV files is generally analyzed in the form of line and scatter plots. These data may be processed with software such as Python, matplotlib, Microsoft Excel, or a text editor such as VSCode. The generated data stored in the Exodus/Nemesis format is commonly analyzed with contour plots of the field variables and material properties. The free software program Paraview is typically used to perform these analyses, sometimes in

conjunction with Python. The data stored in JSON files are generally metadata, and Python or VSCode can be used to analyze the JSON data files.

### 3.3.4 MARMOT

#### 3.3.4.1 Overview

MARMOT is primarily a mesoscale nuclear fuel and structural material performance code implemented using the MOOSE framework. As such, it has application- and material-specific code to simulate the coevolution of microstructure and material properties by coupling the phase field method with solid mechanics, heat conduction and irradiation. MARMOT, an application developed by Nuclear Energy Advanced Modeling and Simulation, requires special permission for access and is made available via the Nuclear Computational Resource Center at INL. The access-controlled code is hosted at <https://github.inl.gov/ncrc/marmot>.

Application-specific models in MARMOT include grain growth and recrystallization, species redistribution and clustering, solid mechanics, heat transfer, phase nucleation, and microstructure reconstruction. Coupling of physics models includes, but is not limited to, grain growth and species interaction, microstructure evolution and solid mechanics, microstructure evolution and heat conduction, microstructure evolution and irradiation, and effective material property determination.

**Table 40. Description of the Data Volume, Associated Software Tools and Other Data for MARMOT Use at INL**

Category	Value
Digital Platform Tag(s)	MARMOT software, git commit hash available
Digital Point of Contact	Larry Agesen, Andrea Jokisaari
Approximate Data Volume per Operation (GB)	1–500, depending on simulation details
Approximate Number of Operations per Year	1,000+
Associated Software Tools	MALAMUTE, MARMOT, MPI, PETSc, libMesh, Paraview, Python, VSCode, matplotlib, CUBIT, Microsoft Excel

#### 3.3.4.2 Data Generation

As with MOOSE, at least three files are required to run a MARMOT simulation: a MOOSE executable binary file, a text-based input file, and an Exodus-based mesh file. Refer to Section 3.3.3.2 for details.

Prebuilt executable binaries for MARMOT are available on INL’s HPC systems Sawtooth and Lemhi with Level 1 user access. Instruction to load the marmot-opt executable and run a text-based input file are outlined in

[https://mooseframework.inl.gov/moose/ncrc/applications/ncrc\\_hpc\\_marmot.html](https://mooseframework.inl.gov/moose/ncrc/applications/ncrc_hpc_marmot.html). Prebuilt executable binaries for installation on a local computer are available via Level 2 user access. Instructions for installation are outline in

[https://mooseframework.inl.gov/moose/ncrc/applications/ncrc\\_conda\\_marmot.html](https://mooseframework.inl.gov/moose/ncrc/applications/ncrc_conda_marmot.html). Mesoscale modeling for additively-manufactured materials will be performed via Source Code Access (Level 4) to MARMOT. Complete source code of the application is available with this access level, which will help develop new capabilities to simulate advanced materials. The minimum

computer system requirements to build the MARMOT executable is the same as that of MOOSE.

### **3.3.5 Data Collection and Transfer, Metadata, and Data Visualization and Analysis**

Refer to Sections 3.3.3.3, 3.3.3.4, and 3.3.3.5 for details as they also apply to MARMOT.

## 4.0 Experimental Equipment and Simulation Tools: ANL

### 4.1 Advanced Manufacturing Equipment

#### 4.1.1 Renishaw AM 400

##### 4.1.1.1 Overview

The Renishaw AM 400 is a single laser powder bed system with a 400 W laser and a 70-micron focal diameter (Figure 27). The build volume is 250 mm by 250 mm by 300 mm. ANL uses this system to print a variety of metal alloy components.



Figure 27. ANL's Renishaw AM 400 Powder Bed Fusion Machine

##### 4.1.1.2 Data Collection

Building parts on this machine follows the standard path of processing an STL geometry into a specific tool path for the machine. ANL uses the Renishaw QuantAM software to do this preprocessing and to specify the machine parameters to be used in the build. One job for the QuantAM slicer is to translate those “global” machine parameters into specific tool commands. For example, while the user might specify some global laser power the actual power delivered to a particular part of the build may vary based on the choices made in the preprocessing software.

In theory, these local machine parameters are available in the actual build files generated by QuantAM and sent to the machine. However, these are in a proprietary format and would require considerable reverse engineering to decipher. For the moment, ANL’s practice is to save the input STL geometry and build files, but only record as metadata the “global” build parameters provided to the QuantAM program along with powder information (size distribution and chemistry).

#### 4.1.1.3 Peregrine and Powder Bed Imaging

ANL is in the process of preparing this machine for use with Peregrine by installing two cameras to monitor the build: a Basler a2A5328-4gmPRO and a Pixelink PL-D734MU-NIR-T. These will provide optical and near infrared imaging of the builds as they are completed. These cameras will provide input to ORNL's Peregrine software, which in turn can be used to detect lack of fusion, abnormal splatter, and other build defects. Based on ORNL's experience we do not plan to archive the RAW camera images, but rather rely on the post-processed Peregrine output for storage.

#### 4.1.2 BeAM Modulo 250

##### 4.1.2.1 Overview

ANL's BeAM Modulo 250 printer is a laser-driven directed energy deposition machine with a build volume of 400 mm by 250 mm by 300 mm (Figure 28). The machine has multiple powder hoppers and a mixing system, allowing ANL to print blended materials with controllable compositions. ANL is in the process of commissioning this machine, and we expect it to be online shortly



Figure 28. ANL's BeAM Modulo 250 Directed Energy Deposition Printer

##### 4.1.2.2 Data Collection

The build process for the directed energy deposition BeAM machine is similar to the PBF Renishaw machine. The input is an STL geometry and a set of global build parameters. Proprietary software made by Siemens (Sinumerik) generate the actual machine G-code. Again, in theory, the full build file could contain useful information but accessing it may require reverse engineering a proprietary file format. So, ANL's plan is to retain the global build parameters specified in the preprocessing software along with the STL geometry and the standard information on the powder chemistry and size distribution.

Unlike the Renishaw machine we have no immediate plans to instrument the BeAM machine with cameras.

Table 41 contains a summary of the information retained by ANL for AMbuilds (or planned to be retained soon).

**Table 41. Data Collected for each AM Build**

Information	Examples	Format	Size
Powder chemistry	16% wt Cr	Compositional analysis (text)	Negligible
Powder size distribution	50 um median powder size	Median size (float) or size distribution curve (float,float)	Negligible
Global build parameters	Laser power 350 W	Text description	Negligible
Ideal build geometry		STL	~10–100 MB
Peregrine annotations		npv	~10 MB per layer, ~1 GB per part

## 4.2 Mechanical Testing and Characterization Equipment

### 4.2.1 Instron Servo-Hydraulic Load Frames

#### 4.2.1.1 Overview

ANL maintains a collection of servo-hydraulic load frames with high temperature furnaces. These load frames are used to determine the strength and reliability of materials at room and elevated temperatures (Figure 29). The exact test conditions and the recorded data vary with test type. These machines can be used for monotonic tension, cyclic (creep or creep-fatigue), or more exotic (e.g., strain rate jump) types of tests.



**Figure 29. An ANL Servo-Hydraulic Load Frame with the Furnace Open**

#### 4.2.1.2 Data Collection and Transfer

Generally, data is a time series of measurements. Typical time series include measurements of time, temperature, strain, and stress. Depending on the test type some of these variables are controlled and some are measured. Test metadata includes sample identifiers, sample dimensions and/or standard sample types, material compositional data, and post-processed test data (for example, elongation to failure. Table 42 summarizes the typical data collected for each test.

The minimum (and maximum) sample size is limited by the capacity of the machine load cell and by test fixturing. As such, these tests tend to capture average, not localized, material data on a large volume of materials.

Table 42. Typical Data Collected in Tests on the ANL Servo-Hydraulic Machines

Information	Examples	Format	Size
Sample metadata	1 in diameter gauge	Text/float	Negligible
Results time series	1 s, 100 C, 2% strain, 100 MPa	CSV/Excel	~1–100 MB, depending on test type

#### 4.2.2 Direct Load and Lever Arm Creep Frames

##### 4.2.2.1 Overview

ANL also has a collection of creep frames, both direct-load and lever arm types (Figure 30 and Figure 31). These machines maintain a constant weight on a sample, held at high temperature in a furnace.



Figure 30. Direct Load Creep Frames



Figure 31. Lever Arm Creep Frames

#### 4.2.2.2 Data Collection and Transfer

Typical measurements, at least at ANL, is a time series of data giving the time, strain, and temperature from the test start to sample failure. We also record metadata, such as the weight/stress on the sample and sample dimensions and post-processed test information such as the creep elongation. Table 43 describes a typical data stream.

Table 43. Typical Data Collected in a Creep Test

Information	Examples	Format	Size
Sample metadata	100 MPa load	Text/float	Negligible
Results time series	1 s, 100 C, 2% strain	CSV/Excel	~1 MB

As with the servo-hydraulic load frames the maximum and minimum test sample dimensions are constrained, and these tests tend to measure the average properties of a fairly large volume of material.

### 4.2.3 Various Box and Tube Furnaces

#### 4.2.3.1 Overview

ANL maintains a collection of box and tube furnaces used to heat treat or thermally age material samples (Figure 32). The data typically collected during the aging parts of thermal aging experiments is limited, typically just the temperature as a function of time.



Figure 32. Some of ANL's Box Furnaces

## 4.2.4 Hysitron TI Premier Nanoindenter

### 4.2.4.1 Overview

Nanoindentation provides a means to measure very local material properties (Figure 33). The direct measurement is a force versus displacement curve applied using a small 1  $\mu\text{m}$ -sized indenter that penetrates a few hundred nanometers into the material. This raw force displacement data can be converted into measurements of the material modulus and hardness. Additionally, the machine can also be used to take in situ scanning probe microscopy images of the surface of the sample.



Figure 33. Hysitron TI Premier Nanoindenter

The key advantage of the nanoindenter is that it provides a means to measure highly local, often sub-grain sized mechanical properties. The hardening measurements often correlate well to room temperature strength. However, the technique is effectively two-dimensional—measuring properties near the sample surface—and, while high temperature systems exist, this particular machine only measures room temperature properties.

#### 4.2.5 Buehler Indenter

#### 4.2.5.1 Overview

The Buehler indenter complements the nano-indenter by providing larger-scale hardness measurements. The raw test data is similar to the nano-indenter—the machine pushes a larger indentation tip into the sample while measuring the force-displacement curve (Figure 34). Again, these measurements can be converted into effective modulus and hardness measurements, which often correlate to room temperature material stiffness and strength.



### Figure 34. Buehler Indenter

The larger indenter size on this machine provides measurements that better correlate to bulk mechanical properties (versus the sub-grain properties provided by the nano-indenter). Again, however, this machine only measures room temperature properties.

#### 4.2.5.2 Optical Microscopes

##### 4.2.5.3 Overview

ANL has access to optical microscopes that can be used for optical metallography on material samples (Figure 35). Interpretation of the data varies depending on how the sample has been prepared (e.g., etching treatment), but the actual test data is a two-dimensional image of a prepared sample. Data size for these images is a few MBs.



Figure 35. One of ANL's Optical Microscopes

#### 4.2.6 FEI Talos TEM

##### 4.2.6.1 Overview

TEM provides extremely high resolution images capturing material microstructure. Image resolutions can be as good as single angstroms, capturing fine details of the material structure such as individual dislocations and fine precipitates (Figure 36).

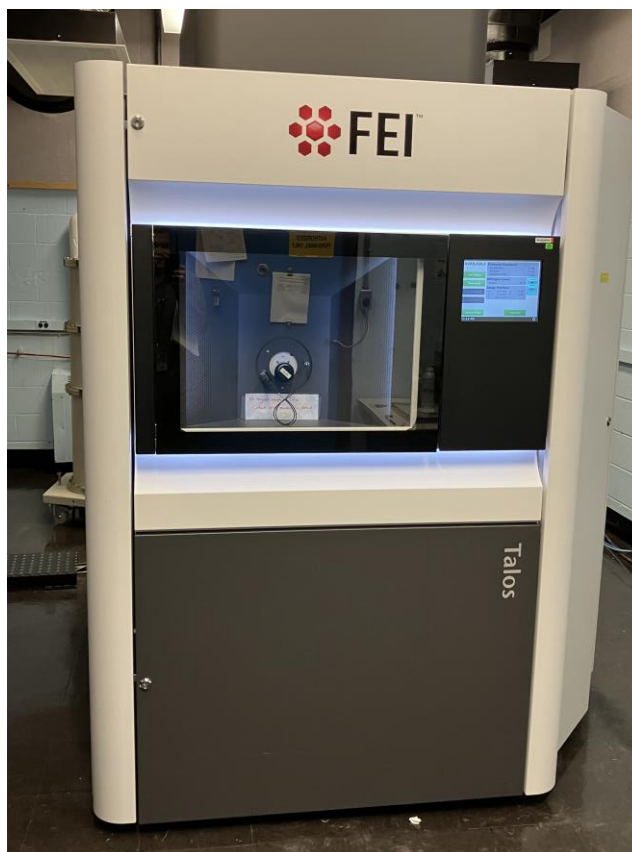


Figure 36. Talos Scanning Transmission Electron Microscope in ANL's Center for Nanoscale Materials

#### 4.2.6.2 Data Collection and Transfer

Raw data for a TEM study is an image (or a series of stitched images) often stored in a .tif format. However, the TEM can also be used to conduct X-ray EDS studies that after processing, produce false color images illustrating the local chemistry of the material. These studies provide information on the local chemical structure of the material; for example, elemental segregation or the composition of second phases.

Images are often on the order of 10 MB, with stitched images having larger sizes.

The main disadvantages of the TEM are the need to prepare special, very thin samples and the limited field of view compared to SEM or optical microscopy.

#### 4.2.7 JEOL JSM-IT800 SEM

##### 4.2.7.1 Overview

SEM offers a wider field of view, compared to TEM but at a lower resolution (Figure 37). Again, the output of SEM studies are often images of the material surface stored as .tif files on the order of 10 MB or larger. SEM can resolve microstructural features like grain boundaries, large precipitates, and coarse dislocation structure. EDS studies are possible to resolve the local chemical composition of the material.

Another viewing option is to use electron backscatter diffraction to study the structure of the material, in particular the material grain structure and crystal orientation. Often, again, this data is post processed into a TIF image or a raw point cloud of data mapping each spatial location to the material phase and crystal orientation. These images are key inputs to microstructural simulations of the material structure.

While much larger the field of view for TEM, SEM studies still cannot survey large areas (Figure 37). Sample preparation is simpler than TEM, though surface preparation may be needed, particularly for EBSD studies.

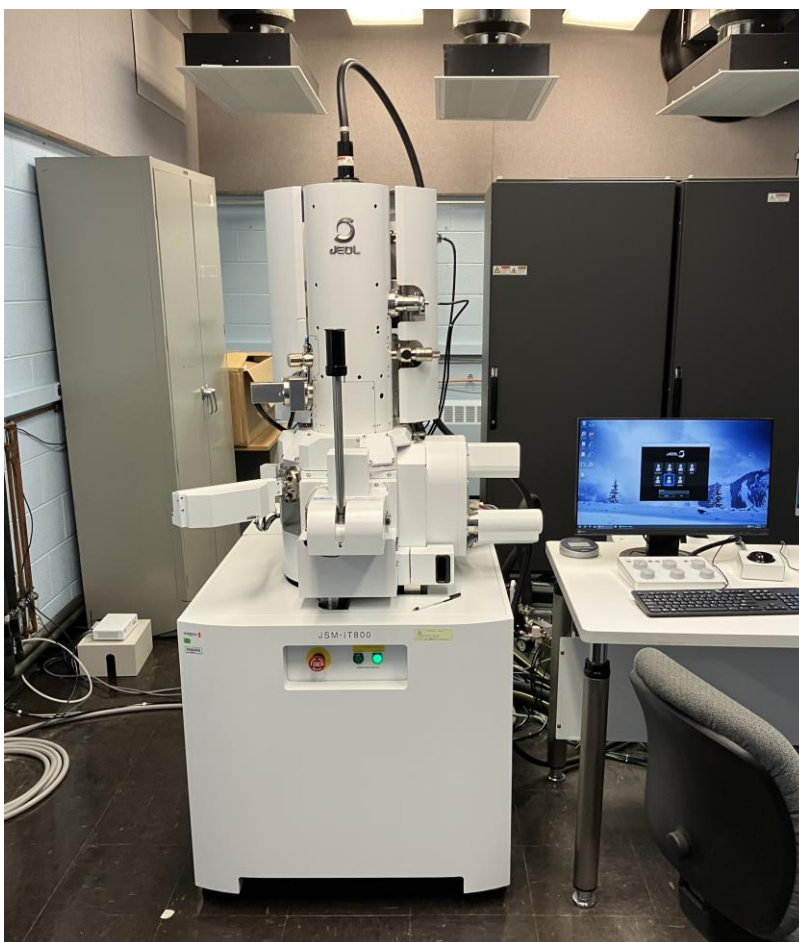


Figure 37. JEOL JSM-IT800 SEM in ANL's Center for Nanoscale Materials

## 4.2.8 The Advanced Photon Source (APS)

### 4.2.8.1 Overview

ANL has a unique capability onsite—the APS. After the upgrade that currently is underway, the APS will be one of the brightest X-ray light sources in the world.

There are many potentially-relevant types of characterization experiments that can be conducted at the APS. This section focuses on three of these techniques: wide-angle x-ray scattering, micron-resolution computed tomography, and high energy diffraction microscopy (HEDM).

#### 4.2.8.2 Wide-Angle X-Ray Scattering

In these experiments, the X-ray beam when interrogating with a crystalline material is diffracted, and the diffraction signal is collected by area detector(s) which can be converted into line profiles for peak analysis (Figure 38). The peak profile contains information about the crystalline phases in the material such as the matrix, precipitates or inclusions. The position and shape of the peaks contain information about the lattice parameter, strain, defect density and coherently scattering domain size of a particular phase.

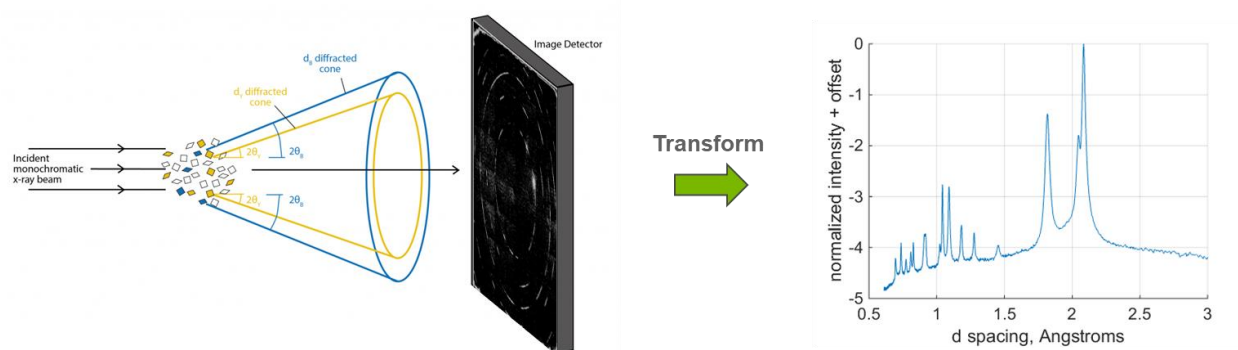


Figure 38. Schematics Showing the Principle of the Wide-Angle X-Ray Scattering Technique Data Collection and Data Processing

#### 4.2.8.3 Micron-Resolution Computed Tomography

The APS is capable of producing tomography images of metallic materials with micron resolution, penetrating through mm or cm thick samples, depending on the specific material (Figure 39). These experiments can resolve small pores and second phases, with sufficient X-ray contrast. Detailed micron measurements of sample porosity could be particularly useful for characterizing additively manufactured material.

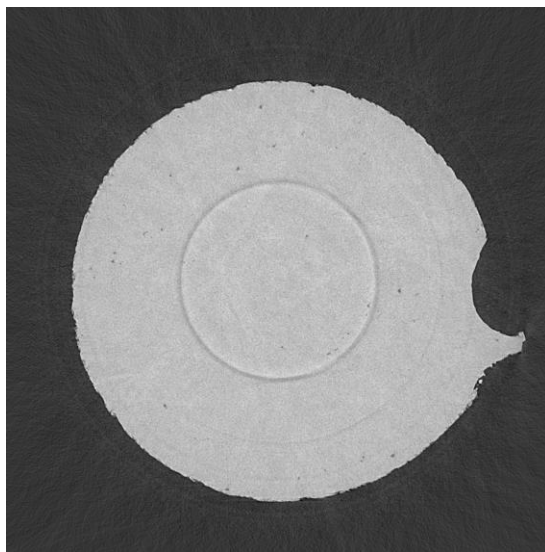


Figure 39. Single Tomography Image from a Stack

The basic output from the experiments is a stack of X-ray image files for slices along one axis of the sample (Figure 40). The .tif format is commonly used and each image can be order 10 MB of data, with thousands of images in a stack, translating to order 10 GB or more of data. These images can be reconstructed to give a 3-D volumetric view of the samples (Figure 40), which contains a comparable amount of data. File formats for reconstructed data are less standardized, though STL descriptions of the sample geometry are one option. From the reconstruction data, information, including size, shape and spatial distribution, about features such as voids, cracks or inclusions can be extracted for quantitative characterization.

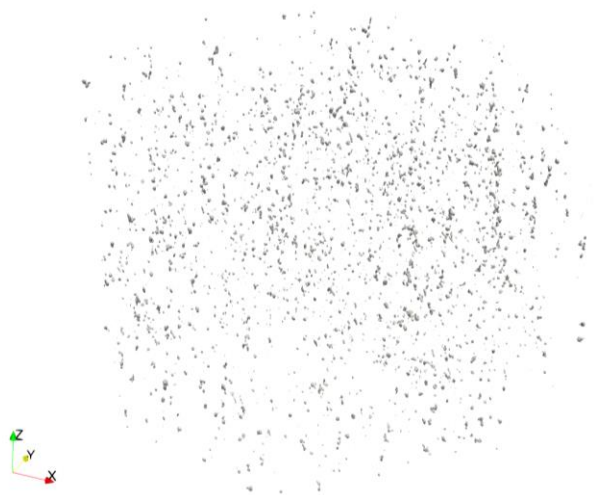


Figure 40. Reconstructed Tomography Dataset (as an STL file) Showing Internal Porosity in a Sample

## 4.2.9 High Energy Diffraction Microscopy

### 4.2.9.1 Overview

HEDM is a means of investigating the microstructure of a sample in three dimensions and in a way amenable to in situ loading during the characterization experiments. HEDM experiments measure the spatially resolved crystal orientation, strain, and grain morphology of a sample in three dimensions. Spatial resolutions can be as accurate as 1  $\mu\text{m}$  in the near field regime.

### 4.2.9.2 Data Collection and Transfer

Processed data is typically a point cloud giving a spatial location associated with a crystal orientation and a strain measure. These points might spatially resolve the material structure (in a near field experiment) or they might indicate grain centroid locations. File formats vary and data from multiple diffraction experiments is often combined into a single point cloud. Storage sizes might be on the order of a few gigabytes, if stored in a text CSV format. Figure 41 shows an example dataset where the point colors indicate the IPF mapped orientation of that region of the material.

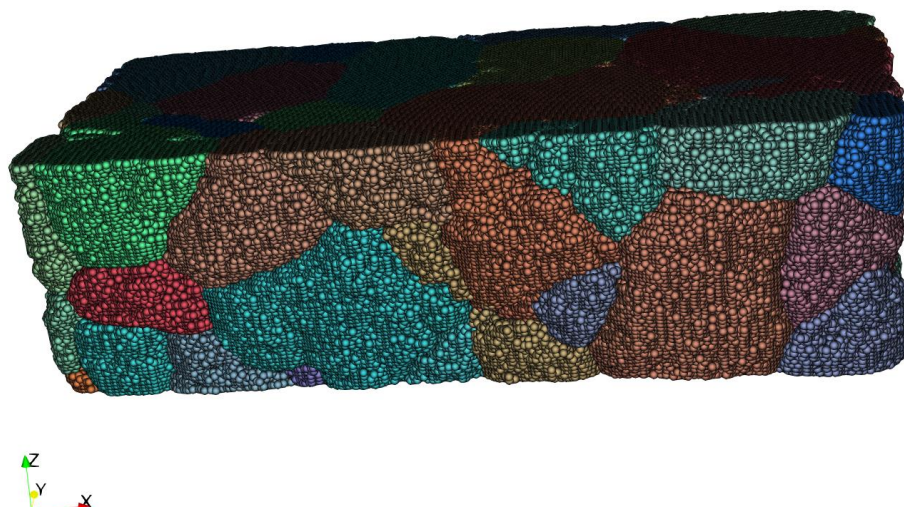


Figure 41. Visualization of a Near Field HEDM Dataset as a Point Cloud of IPF Mapped Grain Orientations

One view of these experiments is that they are a 3-D analog to EBSD experiments in that they provide the grain structure, both morphology and crystal orientation. As these experiments can also provide in situ measurements of strain and reorientation they are a valuable tool in understanding the material deformation mechanisms and validating more detailed models of material behavior.

### 4.3 Materials Modeling Tool

ANL also has modeling and simulation capabilities that could provide input data to the MDDC framework on either macroscale or microscale material properties. These simulations all use the MOOSE framework [1] to provide the underlying finite element solvers and the Nuclear Engineering Materials Library to provide constitutive models. Output data formats are similar for both types of simulations discussed here, providing spatially resolved data (i.e., stress, strain, temperature, composition, etc.) over an unstructured mesh using the ExodusII data format [2]. The difference in the two types of simulations is the spatial resolution. Simulations covering a large volume of material, often an entire component, and more detailed, microstructural simulations resolving only a small volume of material.

#### 4.3.1 Macrostructural Modeling for Residual Stress and Distortion

##### 4.3.1.1 Overview

Macroscale simulations resolving the entire part geometry cannot (easily) predict local material property variations caused by the build processing parameters and the part geometry. However, they can be used to predict the local heat transfer and residual stress and distortion in the component (Figure 42). These simulations might be stored in the MDDC framework to provide estimates of the part distortion, where direct measurements are not available, or to provide input (i.e., maximum temperature or heat flux during the build) for other models.

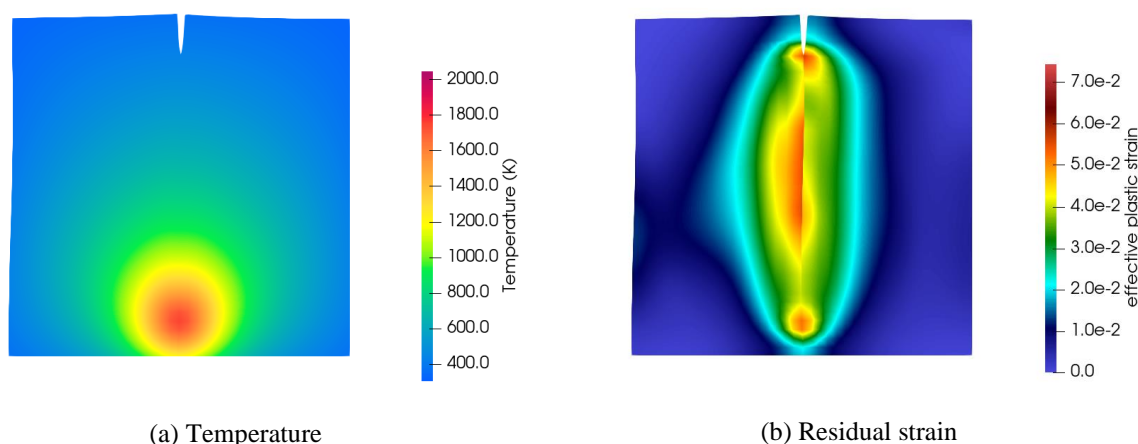


**Figure 42. Example Residual Stress Simulation (here of a weld) Showing Temperature on the Left and Residual Strain on the Right**

Typically, the mesh resolution in macroscale simulations is fairly coarse and final datasets have sizes on the order of tens of gigabytes. On the other hand, postprocessing to reduce the size of the data is seldom useful, as typically the simulations are trying to resolve spatially and temporally varying properties in the build. Some amount of data reduction over time might be useful, for example to find maximum temperatures at a given point.

#### 4.3.2 Microstructural Modeling for Material Properties

Alternatively, the same framework can be used in the context of the crystal plasticity finite element [3] method to resolve the microscale details of the material behavior, as influenced by the material microstructure. The need to resolve the material microstructure in these simulations limits their application to small volumes of material, indexed into a larger AM build. However, these simulations can predict local material properties, accounting for the effect of the local processing conditions on the local microstructure and then the effect of the local microstructure on the effective material properties.

ANL's software focuses on the structure-properties predictions, meaning a complete framework would require processing models mapping from the local processing conditions to the local microstructure.

Figure 43 shows a typical full-field result, which resolves the local stress and strain fields into the material microstructure. These computational meshes are often highly refined and the results integrated over a large number of time steps. The total data can then approach 1 TB in size.

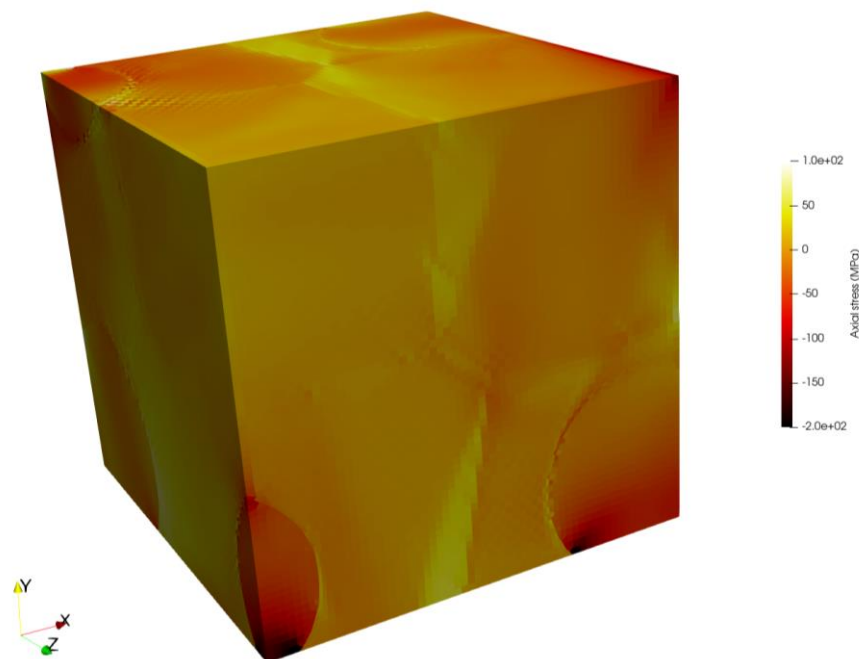


Figure 43. Typical Crystal Plasticity Finite Element Method Simulation of a Composite Material. The fringe colors show the local stress in the loading direction.

However, often these simulations can be postprocessed to greatly reduce the data storage requirements. For example, we may only be interested in the average effective stress strain curve (a time series of scalars) instead of the fully resolved stress and strain fields. However, postprocessing the data and not archiving the full field results does limit future data processing and mining of the simulation data at a future time. Depending on the situation, either the full field results or the postprocessed data might be stored in the MDDC framework.

#### 4.4 Geometric Relational Database

Several of the MDDC framework data storage needs described here are spatial. We would like to associate some type of data with a particular location of a build. For example, a common need in modeling additively manufactured materials is to predict characteristics of the printed part given a set of printing parameters. An effective workflow for developing such models is envisioned below:

1. Print a large batch of samples using different printing parameters.
2. Collect characterization data for the properties of interest for each as-print part.
3. Calibrate numerical models (either those of data-driven, physics-based, or a mix of both) against the calibration data.

There exist a few common challenges using the above workflow, including:

- Data traceability: Every experimental measurement should be tied to a specific part on which the characterization was carried out. This is useful as new characterization techniques are incorporated into the test matrix, especially when material properties are inter-correlated.

- Spatial and temporal variation in the characterization data: Both the printing parameters and the resulting material properties can vary from build-to-build, part-to-part, location-to-location, and even times-to-times.
- Data transferability: In the first two steps of workflow, experimentalists collect the printing parameters and characterization data. In the third step, modelers receive, parse, and reformat the data for modelling purposes. A unified data format reduces the overhead, accelerates the workflow iteration, and avoids interim human error.

This section describes one vision for a geometric relation database structure that could be incorporated on top of the MDDC framework. The idea is to provide “richer” information on the location of specific data within a build and to format the data in a way that makes it easy to do machine learning on the information in the database.

#### 4.4.1 Overview of GeomDB

GeomDB, a geometry-centric relational database, is designed to address the previously mentioned challenges. It is designed with the following key principles:

- Universality: GeomDB allows fully customizable schema to account for any printer.
- Scalability: GeomDB can use GPGPU to manage large datasets with little overhead.
- Flexibility: GeomDB aims for automation by default and provides full control when needed.

GeomDB handles geometry voxelation, location selection, data dependency resolution, checkpoint and reloading, and arbitrary querying operations. Each feature is discussed in detail in the following section.

#### 4.4.2 Software design

In its current version, GeomDB offers the following six modules. The motivation, description, design principles, and design choices for each module are discussed in what follows. For a complete documentation on the library application programming interfaces, please refer to <https://hugary1995.github.io/geomdb/modules.html>

#### 4.4.3 Mesh and voxelization

As the name of the library suggests, a geometry (or its discretized counterpart) is the foundation of the database. Every database built using GeomDB must contain at least one geometry. The mesh module provides geometry definitions and helper functions for conversion between various mesh/geometry formats. GeomDB uses Trimesh (<https://trimsh.org/trimesh.html>) as the geometry and voxelation backend. Because GeomDB is designed with additive manufacturing in mind, STL is currently the only mesh format that has been tested; although, in principle, GeomDB supports any mesh format that is supported by the Trimesh backend.

To better support spatially varying data and location specific database query, a voxelation  $V$  is first created based on the user-provided mesh. Note that a voxelation only approximately represents the original underlying geometry, and the approximation error diminishes as the voxel pitch decreases. Therefore, the user is responsible for choosing an appropriate voxel pitch that can resolve the features both in the part geometry and the spatially varying data. An example is given below in Figure 44 demonstrating the effect of pitch error.



Figure 44. Voxelation of the Stanford Bunny with Three Different Pitches. (Left) pitch = 3, (middle) pitch = 2, (right) pitch = 1.

The voxelation consists of a masking array  $M$  and a transformation matrix  $T$ . The masking array is a 3-D Boolean array in which void voxels have values of 0 and solid voxels have values of 1. The Trimesh backend provides four major types of encodings for the masking array:

1. Dense encoding: the dense representation of the masking array as a three-dimensional array of Boolean values.
4. Sparse encoding: the single-column CSC encoding of the raveled masking array.
5. Run length encoding: sequences of repeated values as the value followed by its count.
6. Binary run length encoding: an optimized form of RLE for when the stored values can only be 0 or 1. This means only counts need to be saved, and assume the values alternate (and start at 0).

Conversions between different encodings are also provided by Trimesh. The transformation matrix is formally termed the 3-D affine transformation matrix: Any combination of translation, rotations, scaling/reflections and shears can be combined in the following  $4 \times 4$  matrix:

$$T = \begin{bmatrix} a_{11} & a_{12} & a_{13} & a_{14} \\ a_{21} & a_{22} & a_{23} & a_{24} \\ a_{31} & a_{32} & a_{33} & a_{34} \\ 0 & 0 & 0 & 1 \end{bmatrix}$$

The transformation matrix is column major in GeomDB. The upper-left  $3 \times 3$  submatrix represents a rotation transform (and optionally scales and shears). The last column represents a translation.  $T$  corresponds to an affine transformation that transforms a point (or vector)  $x$  to another point (or vector)  $y$  by  $y = Tx$ . For a point transformation the fourth elements in the vectors are 1 whereas vector transformation has a 0 (which removes translation operations for vectors).

#### 4.4.4 Locations

As both printing parameters and characterization data can have spatial variations, GeomDB offers a mechanism to select/restrict data to specific volumes/areas of a geometry (or its voxelation). A geometrically defined sub-voxelation is called a location in GeomDB. Recall that the voxelation consists of a masking array and a transformation matrix:

$$V = (M, T).$$

A location  $l$  defines the masking array  $L$  with identity transformation matrix  $I$  (because a sub-voxelation retains the original transformation). Therefore, the sub-voxelation can be written as:

$$V' = (L \odot M, IT) = (L \odot M, T), \quad L = l(V)$$

where  $\odot$  is the element-wise multiplication of two masking arrays. Four primitive locations are implemented in GeomDB:

- Everywhere:  $L = \mathbf{1}$ , where all elements in the masking array are 1.
- Points:  $L = D\left(\left\{\left\lfloor \frac{T^{-1}(x)}{e} \right\rfloor\right\}\right)$ , a collection of voxels that enclose each point, where  $D$  is the dense encoding operator that encodes a set of sparse indices as a dense masking array.
- Bounding box:  $L = (T^{-1}(x) > x_{ll}) \cap (T^{-1}(x) < x_{ur})$ , where  $x_{ll}$  and  $x_{ur}$  define the 3-D rectilinear bounding box.
- Plane:  $L = |\text{dist}(T^{-1}(x), P)| < \text{tol} \frac{\sqrt{3}}{2} \|e\|$ , where  $\text{dist}$  is the signed distance function,  $P$  is the plane parameterized by a point and a normal,  $\text{tol}$  is the tolerance for determining whether a voxel is on the plane, and  $e$  is the pitch.

The Everywhere location is useful in defining location-independent metadata. The other three primitive locations are pictorially illustrated in Figure 45.



Figure 45. Sub-Voxelation Construction Using (left) Points (middle) Bounding Box and (right) Plane

Furthermore, four common operations are supported to compose *composite* locations:

- complement:  $\sim L$ ,
- intersection:  $L_1 \cap L_2$ ,
- union:  $L_1 \cup L_2$ ,
- exclusive union:  $(L_1 \cup L_2) \setminus (L_1 \cap L_2)$ .

The corresponding Python operators are  $\sim$ ,  $\&$ ,  $|$ , and  $\wedge$ , respectively. For example, the negation, intersection, and the union operators are illustrated in Figure 46.

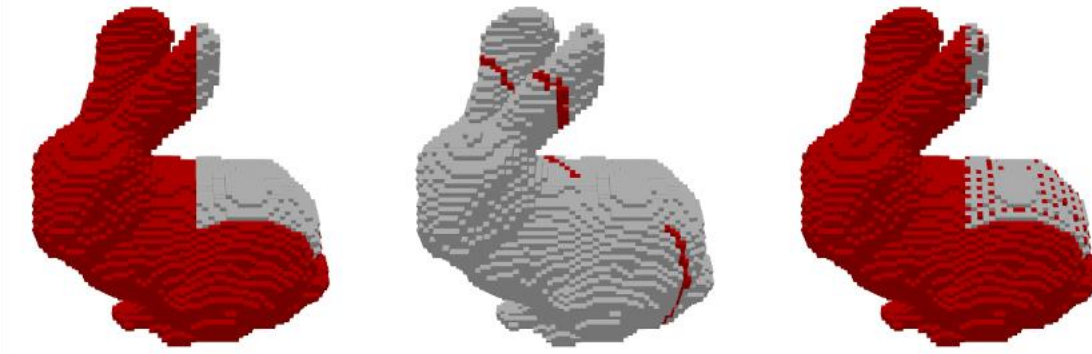


Figure 46. (left) Negation of the Bounding Box (middle); Intersection of the Bounding Box and the Plane; and (right) Union of the Bounding Box and the Points

#### 4.4.5 Conditions

Different data in a relational database can be related to each other. GeomDB supports two types of data relations:

1. The relation in the traditional relational database context expresses a specific data as a function of multiple other data entries.
7. A certain data entry may only be defined on a sub-voxelation where certain conditions are met.

The first type of relation is naturally implemented as part of the Properties evaluation (Section 4.4.6). The second type of relation is called *condition* in GeomDB. Each data entry in the relational database can be associated with multiple conditions. Each condition is parsed from a relational expression which evaluates to a Boolean value, i.e.,  $c: R^n \mapsto \{1, 0\}$ . A data entry is defined on a specific voxel if and only if all the conditions are satisfied at (the centroid of) the voxel. As such, a condition  $c$  also defines a sub-voxelation as:

$$V' = (C \odot M, T), \quad C = c(V, v),$$

where  $C$  is the masking array corresponding to the condition  $c$  and the set of dependent data entries  $v$ .

Similar to the Locations module (Section 4.4.4), composite conditions can be composed using the four common operators: complement, intersection, union, and exclusive union. The utility of conditions is demonstrated in Example 1 (Section 4.4.9).

#### 4.4.6 Properties

The properties module is the main entry point to define data in the database. In GeomDB, a data entry is a named property associated with a location and a set of conditions. A property consists of a location  $l$ , a condition  $c$ , and an expression  $f$  which defines the property value:

$$p = (l, c, f)$$

The location  $l$  of the property can be defined using the Locations module (Section 4.4.4), and the property condition  $c$  can be described using the Conditions module (Section 4.4.5).

When a relational database contains multiple properties, the order in which the properties should be evaluated must be resolved when queries are made. Dependency resolution optimizes and accelerates the query and prevents unstable queries caused by cyclic dependencies. A property  $p_1$  is said to depend on another property  $p_2$  if the evaluation of the condition  $c$  or the expression  $f$  relies on the value of  $p_2$ . GeomDB uses topological sort to resolve the property evaluation order at the beginning of each query, such that by the time each property is evaluated, all of its dependent properties have already been evaluated. If a stable evaluation order cannot be resolved, the user is presented with an error message.

The algorithm for property evaluation is presented below:

1. Given a voxelation  $V = (M, T)$  and all the dependent property values  $\{v_i\}$ , evaluate the location masking array  $L = l(M)$  and the corresponding sub-voxelation  $V_l = (M_l, T) = (L \odot M, T)$ .
2. Set  $V_l^0 = V_l$ . For each dependent property value  $v_i$ , find the sub-voxelation where the dependent property is valid:  $V_l^i = (D(\text{ind}(v_i)) \odot M_l^{i-1}, T)$ . Set  $V_{lv} = V_l^{n_v}$  where  $n_v$  is the total number of dependent properties.
3. Evaluate the condition masking array  $C = c(V_{lv}, \{v_i\})$  and the corresponding sub-voxelation  $V_{lvc} = (M_{lvc}, T) = (C \odot M_{lv}, T)$ .
4. On the resolved sub-voxelation  $V_{lvc}$ , evaluate the current property value  $v = f(V_{lvc}, \{v_i\})$ .

The above algorithm can be repeated for each property according to the resolved evaluation order.

The property in GeomDB only contains the definition of a data entry; that is, how the data entry can be evaluated based on a location and a condition and does not contain the actual data. In fact, the queried dataset may vary, depending on different querying locations. As such, a dedicated object called *property value* is introduced in GeomDB to hold the evaluated data. A property value keeps track of the name of the evaluated property, the (sub-)voxelation on which this property is evaluated, the shape of the voxelation, the sparse indices (CSC format) corresponding to the data entries, and the actual data.

GeomDB also aims to handle the translation from spatially varying database queries to datasets that are readily applicable to machine learning purposes. With that objective in mind, the evaluated property values can also be exported to tables (e.g., Pandas DataFrame) with flattened raveled indices. The data indices are defined in consistency with the voxelation indices:

$$i' = i_x n_y n_z + i_y n_z + i_z,$$

where  $i = (i_x, i_y, i_z)$  is the dense index of the (sub-)voxelation with shape  $(n_x, n_y, n_z)$ .

#### 4.4.7 Database

A relational database in GeomDB consists of one or more voxelations and a set of properties. GeomDB currently supports two types of relational databases: 1) single-geometry (SG) relational database and 2) a replicated-geometry (RG) relational database. Both types of databases contain a single instance of voxelation. They differ only in terms of the data structure of the properties and the evaluation workflow. Figure 47 shows the schematic representation of the data structures of the SG and RG relational databases.

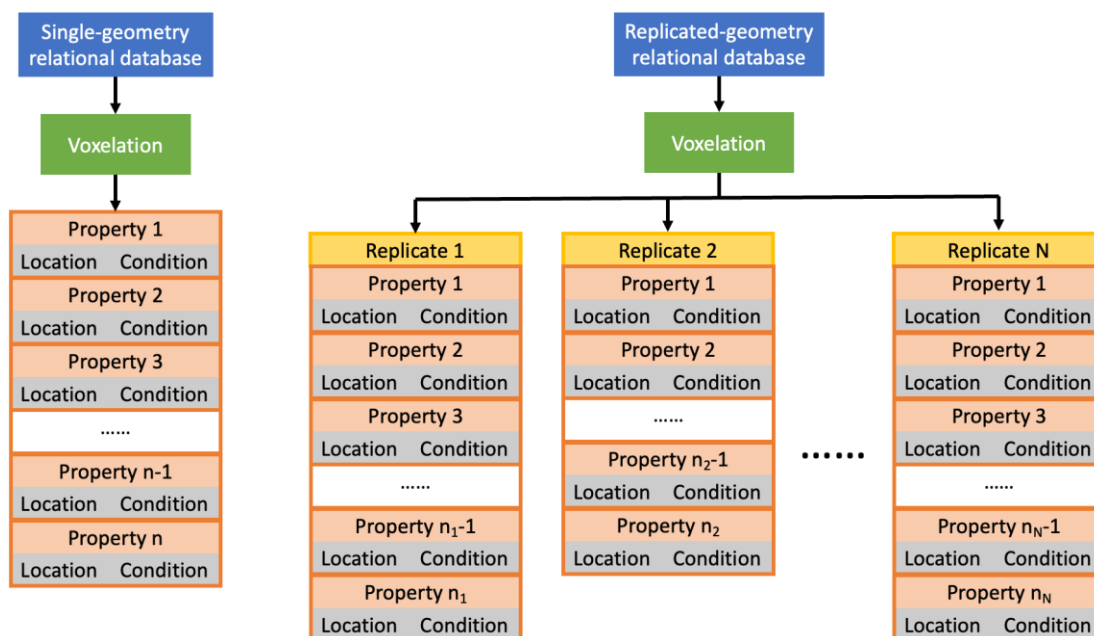


Figure 47. Data Structures of (left) Single-Geometry Relational Database and (right) Replicated-Geometry Relational Database

In an SG relational database, all properties are defined on the same logical geometry. In an RG relational database, however, properties are defined on multiple replicates of a topologically unique geometry. Only a single voxelation is required in an RG relational database, while each replicate of the voxelation maintains their own set of properties. The property types, locations, and conditions can differ from replicate to replicate. The RG relation database is particularly useful in the context of throughput experiments, where many parts with the same geometry are manufactured using different parameters, and characterization of each part proceeds asynchronously.

An SG relational database can be queried with a list of properties and optionally a location. Property dependencies are resolved at the beginning of the query, and the property values are evaluated using the algorithm described above. An RG relational database can be similarly queried with properties and locations. In addition, a list of replicates can be specified to further restrict the query on an RG relational database. Note that property dependencies are resolved per replicate during the query of an RG relational database.

#### 4.4.8 Checkpointing

For ease of curating, managing, and sharing databases, all objects in GeomDB are made *checkpointable*. A checkpointable object is one that can be serialized to and deserialized from a PyTree. The serialization and deserialization utilities are provided by JAX. The terminology PyTree is inherited from the JAX Orbox documentation [4]:

In JAX, we use the term PyTree to refer to a tree-like structure built out of container-like Python objects. Classes are considered container-like if they are in the PyTree registry, which by default includes lists, tuples, and dictionaries. That is: any object whose type is not in the PyTree container registry is considered a leaf PyTree; any object whose type is in the PyTree container registry, and which contains PyTrees, is considered a PyTree.

All types of objects in GeomDB including voxelation, location, condition, property, property value, database, and database query, are checkpointable. Meaning that every intermediate object produced during a database setup, query, or manipulation can be written to a (binary) file, shared among different platforms and devices, and reloaded without loss of information.

#### 4.4.9 Example 1: Single Geometry Relation Database – The Basic Workflow

In this section, the basic workflow for working with databases using GeomDB is demonstrated by creating, saving, and reloading a single-geometry relational database.

First, utility functions are imported from the geomdb namespace; two types of locations, Everywhere and BoundingBox, are imported from the Location module (geomdb.loc); a property of type Constant is imported from the property module (geomdb.prop); the single-geometry relational database of type DataBase is imported from the database module (geomdb.db).

```
from geomdb import *
from geomdb.loc import Everywhere, BoundingBox
from geomdb.prop import Constant
from geomdb.db import DataBase
```

Code Snippet 1 Example 1. Import necessary functions, classes and utilities.

A geometry is then read from a pre-downloaded STL file named “stanford-bunny.stl”, and its voxelation of pitch  $\|a\| = 2$  is created. The voxelation class offers a plethora of useful information, such as the bounds of the underlying voxelation. A sub-voxelation can be created using the bounding box which spans from the lower left corner to the point (31, 3, 49).

```
voxel = voxel_from_stl("data/stanford-bunny.stl", 2)
lower_left_corner, upper_right_corner = voxel.bounds
bb = BoundingBox(lower_left=lower_left_corner, upper_right=[31, 3, 49])
```

Code Snippet 2 Example 1. Read geometry and create voxelation (and a bounding box sub-voxelation).

A single-geometry relational database can be created “on” this voxelation, i.e.,

```
db = DataBase(voxel)
```

Code Snippet 3 Example 1. Create a database “on” the voxelation.

The following code snippet deposits three data entries into the database:

- A property named “a” with constant value “blah” at the location defined by the bounding box.
- A property named “b” with constant value 1.2 at the location complement to the bounding box.
- A property named “c” with constant value metadata –1,000.

```
db.add_property(Constant("a", "blah").at(bb))
db.add_property(Constant("b", 1.2).at(~bb))
db.add_property(Constant("c", -1000))
```

Code Snippet 4 Example 1. Deposit data into the database.

The database now contains three properties named “a”, “b” and “c”. The database is now ready to be queried. For example, the following line of code queries the database for properties named “a” and “c” everywhere.

```
db.query(["a", "c"]).to_dataframe()
```

**Code Snippet 5 Example 1.** Query the values of selected properties.

The query result is output as a table, and a summary of the output is shown in Figure 48.

	index	(a, 0)	(c, 0)	(index, x)	(index, y)	(index, z)	(coord, x)	(coord, y)	(coord, z)
0	5794	blah	-1000	2	15	19	-20.0	-12.0	44.0
1	5795	blah	-1000	2	15	20	-20.0	-12.0	46.0
2	5796	blah	-1000	2	15	21	-20.0	-12.0	48.0
3	5848	blah	-1000	2	16	18	-20.0	-10.0	42.0
4	5849	blah	-1000	2	16	19	-20.0	-10.0	44.0
...	...	...	...	...	...	...	...	...	...
7458	68052	blah	-1000	27	22	17	30.0	2.0	40.0
7459	68053	blah	-1000	27	22	18	30.0	2.0	42.0
7460	68054	blah	-1000	27	22	19	30.0	2.0	44.0
7461	68055	blah	-1000	27	22	20	30.0	2.0	46.0
7462	68056	blah	-1000	27	22	21	30.0	2.0	48.0

7463 rows × 9 columns

**Figure 48.** Example 1 Query Result

The column named “index” lists the unraveled voxel index. The unraveled sparse indices are listed in a two-layer column named “(index, x/y/z)”, and the corresponding voxel centroids are listed as “(coord, x/y/z)”. Finally, the queried data entries are shown in columns labeled with their respective names “(a, 0)” and “(c, 0)”. The dummy index 0 indicates that these quantities are scalars.

The database can be saved, shared, and reloaded on possibly different platforms. The reloaded database will generate the same result with the same query.

```
db.save("overview", override=True)
db_reload = DataBase.load("overview")
db_reload.query(["a", "c"]).to_dataframe()
```

**Code Snippet 6 Example 1.** The database is checkpointable.

#### 4.4.10 Example 2. Replicated-Geometry Relational Database –Real Data with Machine Learning

In this example, a more involved replicated-geometry relational database is created from real experimental data and the available characterization data on additively manufactured 316H cubes. Two machine learning models are then trained to relate specific printing parameters to the average areal porosity.

A voxelation is first created from the STL file of a cube with pitch  $\|a\| = 2$ . A replicated-geometry relational database of type `RGDataBase` is then created on the voxelation.

```
voxel = voxel_from_stl("data/cube.stl", 2)
db = RGDataBase(voxel)
```

##### Code Snippet 7 Example 2. Create the geometry, voxelation, and the RG database

Three types of data are then deposited into the RG database:

- Metadata about the printed parts including homogeneous printing parameters
- Experimentally characterized porosity data
- EBSD scans of three particular parts.

The EBSD scans are generated in the typical CTF format. The scans are preprocessed, segmented, and polished using DREAM3D to identify grains. The lognormal distributions of the grain size and grain neighborhood are then extracted and deposited into the database.

```
renishaw("data/raw.csv")
for file in Path("data/raw").glob("*.csv"):
    db.import_metadata(file, "Sr. No.", exclude=["Source Index"])

db.import_metadata("data/porosity.csv", "ID", prepend_file_name=False)

ids = ["21", "51", "65"]
slice = Plane([-40, 50, 0], [0, 0, 1])
for id in ids:
    stats = segment("data/ebsd/" + id + "/ebsd.ctf", verbose=True)
    size_dist = LognormalStatistics("size_distribution", stats["Volumes"], floc=0)
    neigh_dist = LognormalStatistics("neighbor_distribution", stats["NumNeighbors"], floc=0)
    db.add_property(id, size_dist.at(slice))
    db.add_property(id, neigh_dist.at(slice))
```

##### Code Snippet 8 Example 2. Preprocess and deposit data into the RG database.

To generate the dataset for machine learning purposes, the values of three printing parameters: hatch point distance, hatch power, and hatch exposure time, together with the characterized areal porosity, are queried at a dummy point (for demonstration purposes) on each part.

```

point = Points([[-40, 50, 0]])
results = db.query(
    loc=point,
    prop_names=[
        "scan_volume/Hatches Point Distance",
        "scan_volume/Hatches Power",
        "scan_volume/Hatches Exposure Time",
        "Areal porosity (%)"
    ],
)

```

Code Snippet 9 Example 2. Query certain properties at a single point on all parts.

The query results can be merged and written to a file on disk for distribution, e.g., the queried dataset can be shared with machine learning engineers for training.

```

data = pd.concat(
    [result.to_dataframe(include_coords=False) for result in results.values()]
)
data.to_csv("dataset.csv", index=False)

```

Code Snippet 10 Example 2. Save the query result to a csv file.

In this example, the dataset is used to train a model to predict porosity given the three printing parameters. Two types of neural networks are considered:

1. A deterministic deep neural network with layer sizes 16, 64, 32, 16, 1, and ReLU activation functions
2. A statistical Bayesian neural network with two hidden layers of size 32 and *tanh* activation functions. The neural network weights and biases are sampled from normal distributions of unit variance. A white noise with inverse Gamma distribution with  $\alpha = 1$  and  $\beta = 0.1$  is added to the observation evidence. Markov-chain Monte Carlo simulation is used together with No-U-Turn sampler (NUTS) to infer the posteriors.

One hundred and six porosity measurements are available in the dataset, 58 of which are used to train the machine learning models, and 48 of which are used for validation purposes.

The experimental characterization data and the model predictions are summarized in Figure 49. The data points are plotted in three dimensions with the three printing parameters as the axes. The data points are colored using the log of the areal porosity percentage. The confidence in the predictions made by the statistical model is plotted in the lower right corner of the figure.

Finally, the effectiveness of the statistical model is validated by applying it on the unseen 48 data points (Figure 50). Combinations of the three printing parameters are used to label the horizontal axis without ordering. The scatter points are ordered such that the mean predictions are in the ascending order. The mean predictions are plotted as the black solid line. The plus/minus standard deviation and the 5%/95% posterior percentiles are plotted as dark gray and light gray bands, respectively. The purple crosses mark the 58 data points used in the training process, and the 48 unseen data points are marked in red.

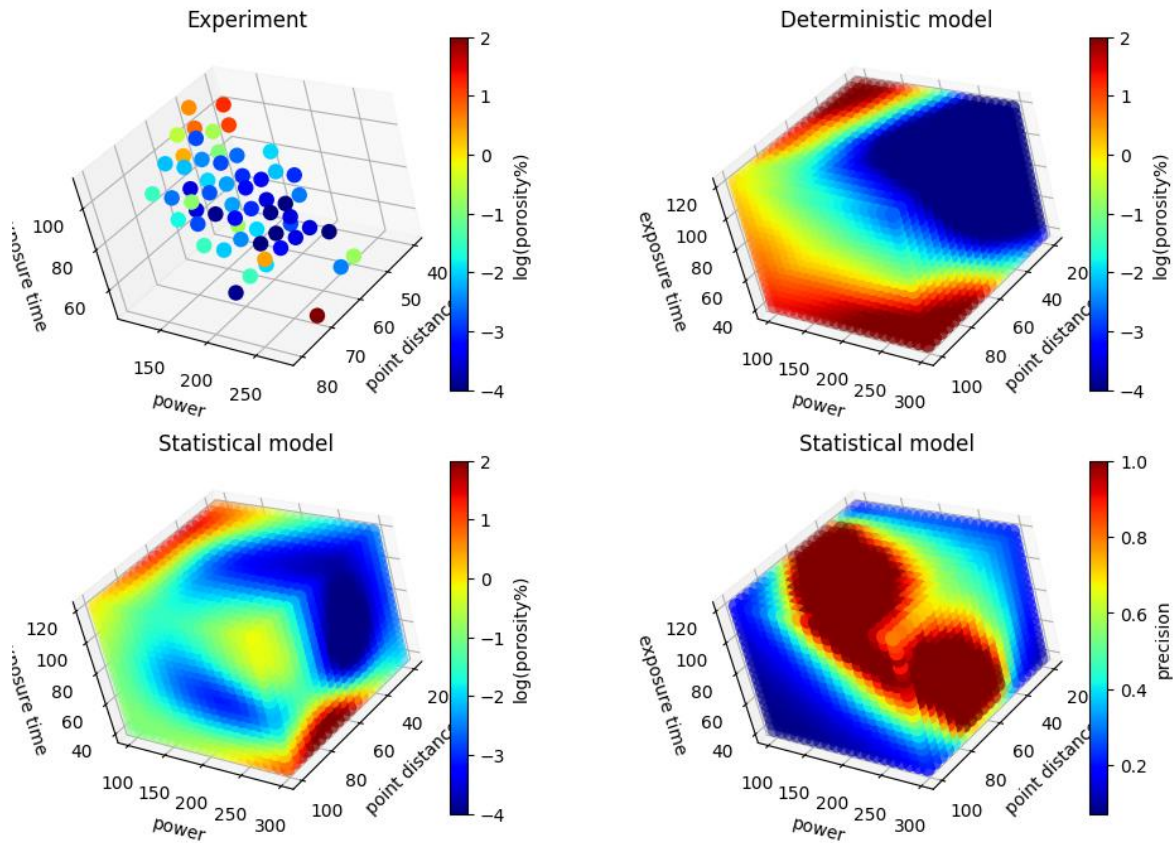


Figure 49. Example 2: Experimental Data and Model Predictions

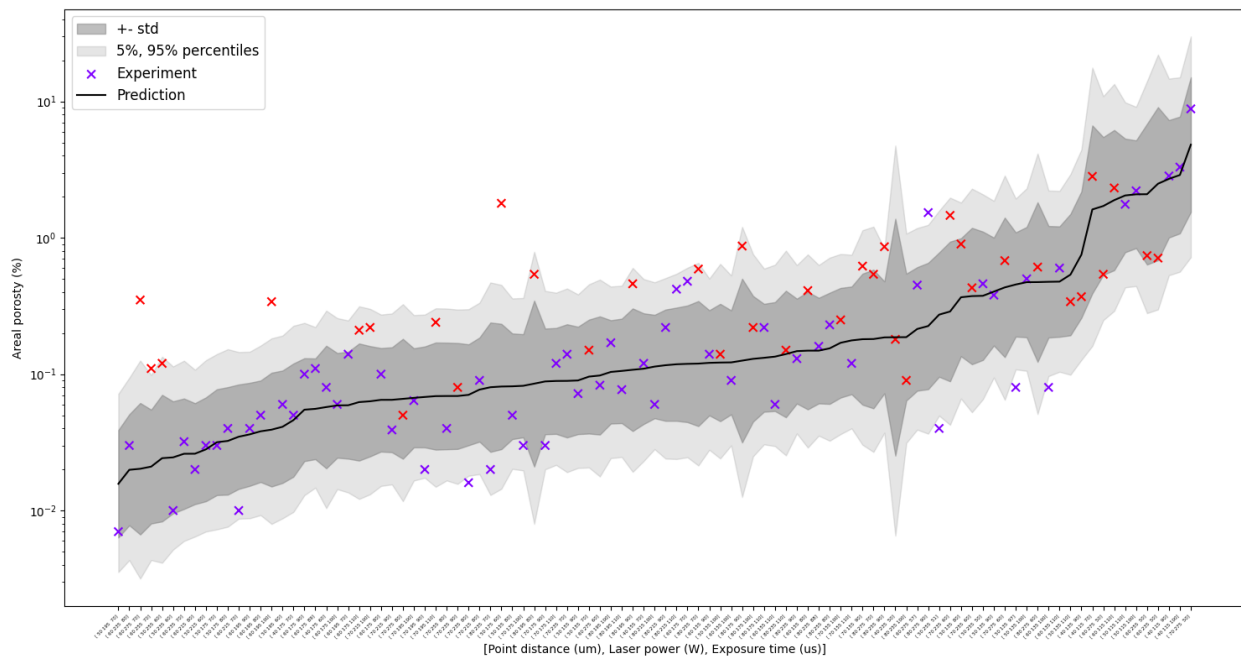


Figure 50. Example 2: Validation of the Inferred Statistical Model Against the 48 Unseen Data Points

## 5.0 Experimental Equipment and Simulation Tools: LANL

### 5.1 Advanced Manufacturing Equipment

#### 5.1.1 EOS 400 M 400

##### 5.1.1.1 Overview

The EOS M 400 is a metal 3-D printer produced by EOS. It uses the Direct Metal Laser Sintering technology (Powder bed fusion type method) to produce aluminum, copper, inconel, steel and titanium parts using powder feedstock (Figure 51). This is a large volume printer capable of printing object with dimensions 400x400x400mm. The minimum layer thickness is 0.09 mm. The EOS M400 is used in conjunction with EOS softwares. In particular, EOS Build/Build+ is a parameter editor allowing to control all process parameters such as build speed, surface finish. The tool is equipped with a Material Set Management capability to rapidly perform new builds with known feedstock. In parallel, EOS Smart Monitoring a smart Monitoring tool that uses optical tomography for process insights. A high-resolution near-infrared camera records and measures the energy input in real time. Automated feature can adjust laser power levels to optimized specifications established in pre-processing, making corrections during the build as needed.



Figure 51. EOS M400-1 3-D Printer

#### 5.1.2 Data Collection and Transfer

- Build Volume: 400 x 400 x 400mm;
- Max Power: 380W
- Materials: Stainless Steels, Ti64, Ti5553, Ta, W, Inconel 625 & 718, Tool Steels 4340 & 8620, Al A20X & AlSiMg10, TZM
- Scan speed up to 7.0 m/s (23 ft/s)
- Laser Type: Yb-fiber laser; 1,000 W

#### 5.1.3 Data Visualization and Analysis

The data associated with each build can be extracted in CSV format and thus be integrated within any data framework (SQL, Python). The two primary softwares (BUILD+ and Smart

Monitoring), store all data associated with pre-processing, build geometry, build parameters (e.g., laser power, scan rate) and optical data generated during the build.

## 5.1.4 EOS 400 M 290

### 5.1.4.1 Overview

The EOS M 290 is a metal 3-D printer produced by EOS (Figure 52). It uses the Direct Metal Laser Sintering technology (Powder bed fusion type method) to produce aluminum, copper, inconel, steel and titanium parts using powder feedstock. This is a moderate sized volume printer capable of printing object with dimensions 250 x 250 x 325mm. The minimum layer thickness is 0.09 mm. The EOS M290 is used in conjunction with EOS softwares. In particular, EOS Build/Build+ is a parameter editor allowing to control all process parameters such as build speed, surface finish. The tool is equipped with a Material Set Management capability to rapidly perform new builds with known feedstock. In parallel, EOS Smart Monitoring a smart Monitoring tool that uses optical tomography for process insights. A high-resolution near-infrared camera records and measures the energy input in real time. Automated feature can adjust laser power levels to optimized specifications established in pre-processing, making corrections during the build as needed.



Figure 52. EOS M400-1 3-D Printer

### 5.1.4.2 Data Collection and Transfer

- Build Volume: 250 x 250 x 325mm
- Max Power: 380W
- Materials: Stainless Steels, Ti64, Ti5553, Ta, W, Inconel 625 & 718, Tool Steels 4340 & 8620, Al A20X & AlSiMg10, TZM
- Scan speed up to 7.0 m/s (23 ft/s)
- Laser Type: Yb-fiber laser; 380 W
- Focus diameter 100  $\mu$ m (0.004 in)

#### 5.1.4.3 Data Visualization and Analysis

The data associated with each build can be extracted in CSV format and thus be integrated within any data framework (SQL, Python). The two primary softwares (BUILD+ and Smart Monitoring), store all data associated with pre-processing, build geometry, build parameters (e.g., laser power, scan rate) and optical data generated during the build.

## 5.2 Mechanical Testing and Materials Characterization Equipment

### 5.2.1 Creep Testing

#### 5.2.1.1 Overview

The Zwick 5-axis Creep Tester applies a mechanical load on up to five samples using five independent axes in a temperature- and humidity-controlled environment to measure various mechanical properties (Figure 53). By measuring the crosshead displacement, time, and temperature, stress versus strain curves and creep curves (strain versus time) can be produced. Analysis of this data within the program can be performed to calculate materials properties such as modulus and strength using the raw test data and sample geometry measurements. Custom calculations can also be made for determining other values of interest that are not already available within each program. It also features a video extensometer for tracking displacement of the sample directly on the sample surface by tracking two points. A digital image correlation system is also available that can be used to calculate strain over the entire sample surface independent of the load frames.



Figure 53. Zwick Roll Creep Testing Machine

The raw load is the amount of force applied in tension or compression to a sample. The crosshead displacement is the distance the crossheads have moved after applying a load relative to their initial location. The temperature of the sample and the time since the load was first applied are exported each time the raw load and crosshead displacement are exported.

#### 5.2.1.2 Data Collection and Transfer

- The Zwick Creep Tester exports raw load, crosshead displacement, time, and temperature data.
- Test Speed: 0.001 mm/h to 100 mm/h; speed accuracy: 0.1% ; travel resolution: 0.0025  $\mu\text{m}$  ; force and strain control of 1,000 Hz.
- Default metadata captured includes Customer, Test Standard, Material Type, Specimen Type, Pre-Treatment, Tester, Machine Data, Specimen I.D., Specimen Dimensions, Date. Metadata capture can be configured to capture any additional parameters.

#### 5.2.1.3 Data Visualization and Analysis

- The data file consists of columns of data with a header row specifying the data in each column.
- The data file can be manipulated to include any number of values laid out in any order, and custom reports can also be made for any test procedure ran. The data can include raw load, crosshead displacement, time, temperature, stress, and strain.
- The data is exported as a CSV, Excel, or text file, and is therefore read using Excel, a text editor, or any other scripting language capable of importing these file types.

### 5.2.2 Mechanical Testing: Tension and Compression 1

#### 5.2.2.1 Overview

The MTS Insight 30 is a single axis electromechanical load frame equipped with an environmental chamber (Figure 54).



Figure 54. MTS Electromechanical Load Frame

The MTS Insight applies a mechanical load in tension or compression to measure the mechanical properties of a material. The environmental chamber can be used to control the temperature at which the mechanical testing is performed. A digital image correlation system is also available that can be used to calculate strain over the entire sample surface independent of the load frame. Data analysis can be performed within the program for the frame to calculate and make plots such as stress and strain curves, as well as calculate material properties including modulus and strength using the raw test data and sample geometry measurements. Custom calculations can also be made for determining other values of interest that are not already available within each program.

### 5.2.2.2 Data Collection and Transfer

- The raw load (mechanical load applied), crosshead displacement, and time are all recorded during a run.
- The raw load is the amount of force applied in tension or compression to a sample. The crosshead displacement is the distance the crosshead has moved relative to its initial location. The time since the data acquisition was triggered is exported each time the raw load and crosshead displacement are exported.
- Position Resolution: 0.001 mm (0.00004 in.)
- Position Accuracy: 0.01 mm (0.0004 in.)
- Sampling Rate: 1,000 Hz
- Maximum Load: 30 KN.

### 5.2.2.3 Data Visualization and Analysis

- The data file consists of columns of data with a header row specifying the data in each column. It can be manipulated to include any number of values laid out in any order. Custom reports can also be made for any test procedure ran.
- The data is exported as a CSV, Excel, or text file, and is therefore read using Excel, a text editor, or any other scripting language capable of importing these file types. A report summarizing the calculations and graphs, such as a stress versus strain curve, made with the software can also be generated. This report can be exported in PDF or Excel format.
- Commonly used metadata variables are Test ID, Specimen ID, Date, Sample Dimensions, and Operator. Custom metadata variables can be made and added to any test configuration and/or report template.

## 5.2.3 Mechanical Testing: Tension and Compression 2

### 5.2.3.1 Overview

The MTS Criterion 43 is a single axis electromechanical load frame soon to be equipped with an environmental chamber (Figure 55). The MTS Criterion applies a mechanical load in tension or compression to measure the mechanical properties of a material. The environmental chamber can be used to control the temperature at which the mechanical testing is performed. A digital image correlation system is also available that can be used to calculate strain over the entire sample surface independent of the load frame. Data analysis can be performed within the program for the frame to calculate and make plots such as stress and strain curves, as well as calculate material properties including modulus and strength using the raw test data and sample

geometry measurements. Custom calculations can also be made for determining other values of interest that aren't already available within each program.



Figure 55. MTS Criterion 43 electromechanical load frame.

#### 5.2.3.2 Data Collection and Transfer

- The raw load (mechanical load applied), crosshead displacement, and time, are all recorded during a run.
- The raw load is the amount of force applied in tension or compression to a sample. The crosshead displacement is the distance the crosshead has moved relative to its initial location. The time since the data acquisition was triggered is exported each time the raw load and crosshead displacement are exported.
- Sampling Rate: 1,000 Hz
- Position Accuracy: within  $\pm 0.5\%$
- Strain Accuracy: ASTM E83 or ISO 851.

#### 5.2.3.3 Data Visualization and Analysis

- The data file consists of columns of data with a header row specifying the data in each column. It can be manipulated to include any number of values laid out in any order. Custom reports can also be made for any test procedure ran.
- The data is exported as a CSV, Excel, or text file, and is therefore read using Excel, a text editor, or any other scripting language capable of importing these file types. A report summarizing the calculations and graphs, such as a stress versus strain curve, made with the software can also be generated. This report can be exported in PDF or Excel format.

- Commonly used metadata variables are Test ID, Specimen ID, Date, Sample Dimensions, and Operator. Custom metadata variables can be made and added to any test configuration and/or report template.

## 5.2.4 Mechanical Properties Characterization at High Temperature

### 5.2.4.1 Overview

The Gleeble 1500/20 is a helpful tool for a wide variety of materials research programs (Figure 56). It is a full digital control system that allows testing the response of materials under high thermo-mechanical loads with accurate control of thermal and mechanical parameters as well as smooth transitions in thermal and mechanical loads. Applications include the study of weld heat affected zones, hot ductility, melting and controlled solidification, phase transformation studies as well as various heat treatment studies. The Gleeble can measure stroke and load and generate stress and strain curves. It can be used to assess if the deformation is stable or unstable or if annealing is needed to produce stable deformation. This specific Gleeble set up can test materials at temperatures reaching 3,000°C.



Figure 56. Gleeble 1500

### 5.2.4.2 Data Collection and Transfer

The data collected consists of stress, strain curves and of temperature time curves.

- Maximum compressive force: 10 metric tons
- Maximum Stroke distance: 100 mm
- Maximum Stroke rate: 1,000 mm/sec
- Maximum temperature: 3,000°C
- Maximum Heating and quenching rate: 10,000°C/sec
- Maximum specimen size: 20 mm

### 5.2.4.3 Data Visualization and Analysis

The data can be visualized using either excel or python.

## 5.2.5 Microstructure Characterization: Scanning Electron Microscope 1

### 5.2.5.1 Overview

The JEOL JSM-IT 100 is a scanning electron microscope (SEM) equipped with several detectors (ETD, BSD, LVD) allowing for a wide range of imaging pressures (Figure 57). The tool also has electron dispersive x-ray spectroscopy (EDS) capabilities. It takes images of a sample's surface using an electron beam in a controlled environment. EDS allows the user to perform elemental analysis of the sample surface.



Figure 57. JEOL JSM-IT 100 Scanning Electron Microscope

### 5.2.5.2 Data Collection and Transfer

- Micrographs by secondary or back scatter electron imaging and EDS maps/spectra.
- The data provides microscale morphology and elemental composition.
- In the best case, the tool resolves to ~10 nm. Typical resolution is ~50nm.

### 5.2.5.3 Data Visualization and Analysis

- .tif or .pdf
- The data is read using an image software or pdf viewer.
- The image condition data bar is collected as part of the image.

## 5.2.6 Microstructure Characterization: Scanning Electron Microscope 2

### 5.2.6.1 Overview

The Thermofisher FEI Quattro S is an environmental scanning electron microscope (SEM) equipped with several detectors (ETD, CBS, ABS, GSED, LVD) allowing for a wide range of imaging pressures (Figure 58). The tool also has electron dispersive x-ray spectroscopy (EDS) capabilities. It takes high resolution images of a sample's surface using an electron beam in a controlled environment. EDS allows the user to perform elemental analysis of the sample surface.



Figure 58. Environmental Scanning Electron Microscope Equipped with Several Detectors (ETD, CBS, ABS, GSED, LVD)

### 5.2.6.2 Data Collection and Transfer

- Micrographs by secondary or back scatter electron imaging and EDS maps/spectra.
- Microscale morphology and elemental composition.
- In the best case, the tool resolves to ~1 nm.

### 5.2.6.3 Data Visualization and Analysis

- .Tif or .esma (much like .csv).
- Image software or excel.
- The .esma file captures information such as sample collection date & time, owner, units of the EDS spectrum, beam conditions (angle, current, position), pressure, detector information (gain, count rate, dwell time, deadtime), and crystal information.

## 5.3 Materials Modeling Tool

### 5.3.1 Micron-scale Simulations

#### 5.3.1.1 Overview

Los Alamos National Laboratory has developed a discrete dislocation dynamics (DDD) tool coupled with both a chemo-mechanical solver and a phase field modeling capability (Figure 59).

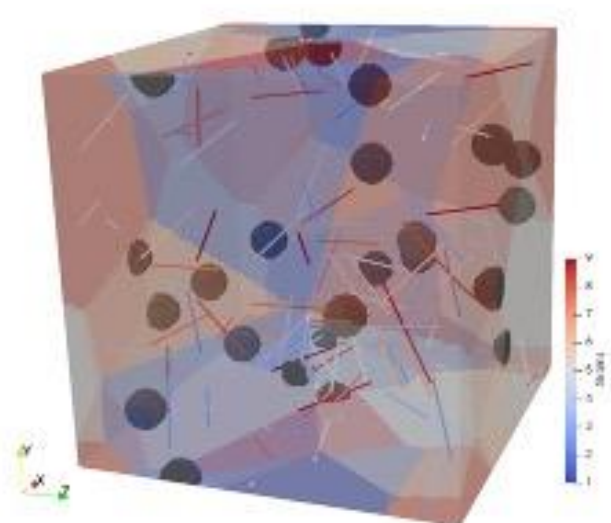


**Figure 59.** Example of Microstructure Configuration Generated by DDD. The specific configuration shown corresponds to a small grain polycrystal containing dislocation lines and precipitates (size ~10nm).

Key to these methods lies the utilization of Fast Fourier Transform solvers for both mechanical and chemical fields. The DDD tool allow for the simulation of the plastic strain and its rate resulting from the collective motion and interactions of dislocation with obstacles (e.g., voids, bubbles, precipitates and other dislocations) in single crystals or oligocrystals. Uniquely, the DDD method keeps track of the two-way coupling between point defects and dislocations such as to predict the activity of dislocation climb as a function of temperature and irradiation conditions. Further, the DDD tool can quantify the effects of free surfaces on both mechanical fields and dislocation configuration changes. The DDD code can simulate complex mechanical loading scenarios (i.e., multi-path, temperature ramps). Finally, the DDD tool can also quantify

the diffraction signature resulting from the elastic strain within the sample; thereby allowing for a model-assisted interpretation of diffraction signals.

Over the past decade this numerically efficient code was used with success to quantify the coupled effects of one-dimensional, two-dimensional, and 3-D defects on materials strength, to quantify the kinetics of dislocation recovery, to quantify the strengthening effects of non-shearable precipitates on slip in face center cubic crystals. In the context of the AMMT program, DDD could be used to unravel the roles of dislocation cells on creep and to build models for the evolution of these cell structures. DDD can also be coupled to thermodynamic models to develop predictors of time-temperature-precipitation with sensitivity to the internal stresses within the material.

### 5.3.1.2 Data Collection and Transfer

Overall, the DDD code outputs data related to the dislocation content at each point, mechanical fields (elastic and inelastic strains and their rates, Cauchy stress). The DDD code generate data associated with the mechanical response and evolution of the state of microstructure of single and polycrystals. The list below details typical characteristics of these simulations.

- Simulation volume: Up to 1.5 micron cube
- Strain rates:  $1\text{e-}15/\text{s}$  up to  $1\text{e}5/\text{s}$
- Temperature range: 0K to melting temperature
- Mechanisms: Slip, climb, cross-slip
- Crystal structure that can be simulated: fcc, bcc, hcp.

For each simulation, one can elect to output field or spatially average data every  $n$  times steps.

### 5.3.1.3 Data Visualization and Analysis

Average data are produced in the form of text and csv files that can be read with any Python-like scripts. The code comes equipped with post-processor allowing to automatically plot the average mechanical response, dislocation density evolution and contributions from slip, climb and glide. The field data are generated in the \*.vtk format. The software paraview is typically used to visualize and analyze the data.

## 5.3.2 Thermodynamic Simulations

### 5.3.2.1 Overview

Within the course of AMMT, a new modeling tool is being developed. It aims at predicting the kinetics of precipitation in the presence of complex multi-directional stress fields. The tool is under development and will essentially enhance the predictive capabilities of commercially available softwares. As inputs the model will necessitate access to thermodynamic and kinetic databases. Simulations rely on the use of Eshelabian micromechanics to quantify the evolutions of the Gibbs free energy of configurations containing precipitates and dislocations. As such, the model requires as input an initial defect content, the imposed temperature and the desired simulation time. It outputs a simple csv file detailing as a function of time the types of precipitates present, the number density of each precipitates as well as the size of precipitates.

The tool needs to be connected/plugged into existing Gibbs minimizers themselves connected to databases. Databases for 316 steels have already been developed throughout the literature.

### 5.3.2.2 Data Collection and Transfer

The model will generate simple csv files detailing time, temperature, precipitate type, number density and size of precipitates. Per simulation, the data will not exceed a few hundred kb.0.

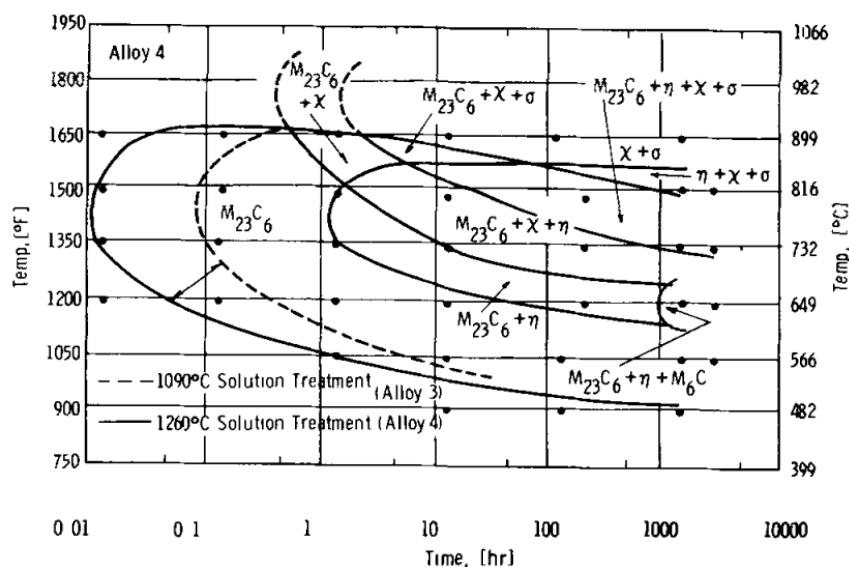


Figure 60. Experimental Time Temperature Precipitation Diagram for 316L Steel. The tool under development will produce similar plots as shown here.

### 5.3.2.3 Data Visualization and Analysis

The model will produce \*.csv files that can be analyzed via the use of simple python scripts.

## 5.3.3 Polycrystal Plasticity Simulations: LAPx

### 5.3.3.1 Overview

The Los Alamos Polycrystal code (LAPx) predicts the mechanical response of crystalline materials subjected to arbitrary quasi-static (i.e., low strain rates) scenarios. LAPx uses fast Fourier transform based methods to solve for the stress and strain states at each point within a complex microstructure. Uniquely, this capability predicts the relative and absolute contributions of all plastic deformation mechanisms activated during loading. These mechanisms include dislocation glide, dislocation climb, vacancy diffusion processes (i.e., diffusion along grain boundaries and within the bulk, effect of non-equilibrium point defects due to irradiation), and porosity evolution due to damage.

The LAPx code solves the mechanical equilibrium condition in a voxelized microstructure. Key to it is the use of a fast Fourier transform based algorithm to rapidly quantify the stress and strain fields at each point. Further, the code is equipped with several advanced constitutive equations which relate the inelastic strain at each point to both stress, temperature and features of the microstructure (i.e., dislocation content, precipitate content, local porosity). All of these

features of the constitutive equations have been the subject of either reports or publications available in the open literature.

As shown in Figure 61, Lapx can simulate the variability in performance (in this example, the steady state creep rate at a given temperature) as a function of the details of a microstructure (including precipitates, dislocations, grain size, morphology). Currently, the code can perform several thousand simulation leveraging commonly available high performance computing resources (i.e., 32 CPUs for 5 days).

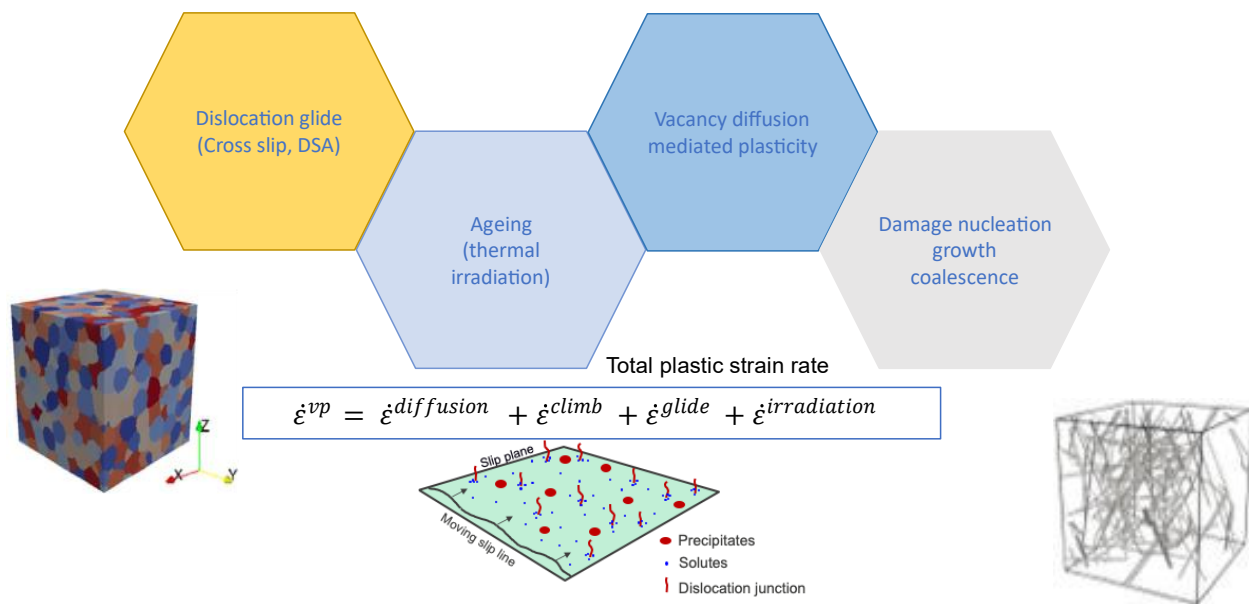


Figure 61. Constitutive Modeling Modules Available within Lapx

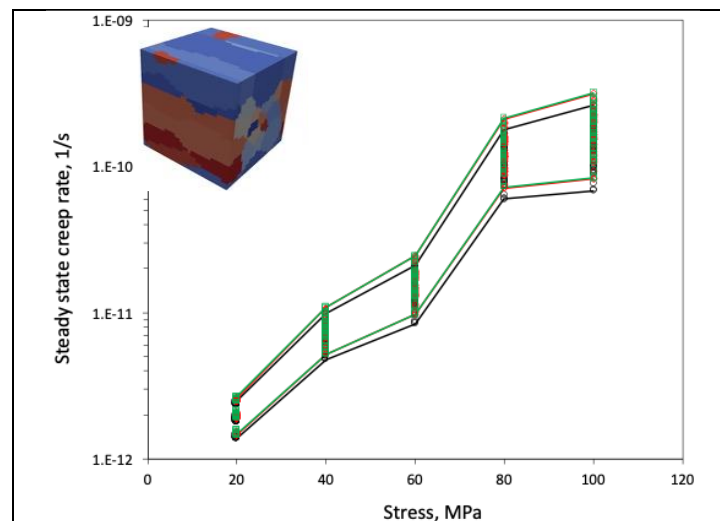


Figure 62. Predicted Envelope of the Steady State Creep Rate of 316H Processed by AM. Temperature is 650°C. The microstructure was varied as a function of precipitate size and density, dislocation content, porosity and grain aspect ratio.

### 5.3.3.2 Data Collection and Transfer

LApX produces two types of datasets respectively associated with average quantities and with field data. Average quantities detail the overall mechanical response of the materials (i.e., elastic strain, plastic strain, average contribution of each deformation mode, stress), the state of microstructure (e.g., porosity at each time step, dislocation density on each slip system), and metadata associated with the input decks and convergence performance of the code. Overall, a typical creep simulation (e.g., 20 years of performance) would generate a few hundred kb of average data. All of which is written in a series of csv files. Field data are written under the hdf-5 format. The size of the dataset depends on both desired output frequency and number of points used to compute mechanical fields. The typical number of Fourier points ranges from 323–1,283.

### 5.3.3.3 Data Visualization and Analysis

Data are typically visualized and analyzed using python scripts and paraview.

## 5.3.4 Surrogate Models: LAROMance

### 5.3.4.1 Overview

LAROMance is a suite of data-driven models predicting the mechanical response of several structural engineering metals subjected to extreme environments. These models are integrated into finite element solvers and allow for the simulations of the response of engineering structures as a function of the microstructure of the metal.

The overall goal is to enable an end user to use high performance computing clusters to perform structural simulations in a matter of hours (or days at most). To date, engineering approaches favor the numerical efficiency of models to the detriment of their predictiveness. In consequence, current engineering type models are not adequate to quantify the effects microstructure, temperature and stress transients, irradiation effects on mechanical performance. Opposite to this, the mechanics of materials community has for decades aimed to develop and validate advanced constitutive models which can be used to extrapolate how microstructure composition and time evolving loads will affect both microstructure evolution and mechanical response (cf LApX). These however rarely can be utilized for engineering applications due to their numerical cost and overall complexity. LAROMance builds a bridge between these two communities.

LAROMance constitutive laws are derived from mining databases of predictions emanating from the use of highly complex microstructure sensitive models of the response of polycrystals (LApX). LAROMance laws can replicate predictions from LApX at the fraction of the numerical cost. Thus far, LAROMance offers constitutive models for a wide panel of metals of critical importance to the energy industry: Gr91, HT9, 316H, 347H. HT9 for example, is a ferritic steel with outstanding mechanical performance and resistance to irradiation. The LAROMance constitutive models have been embedded in two finite element softwares; MOOSE and Abaqus.

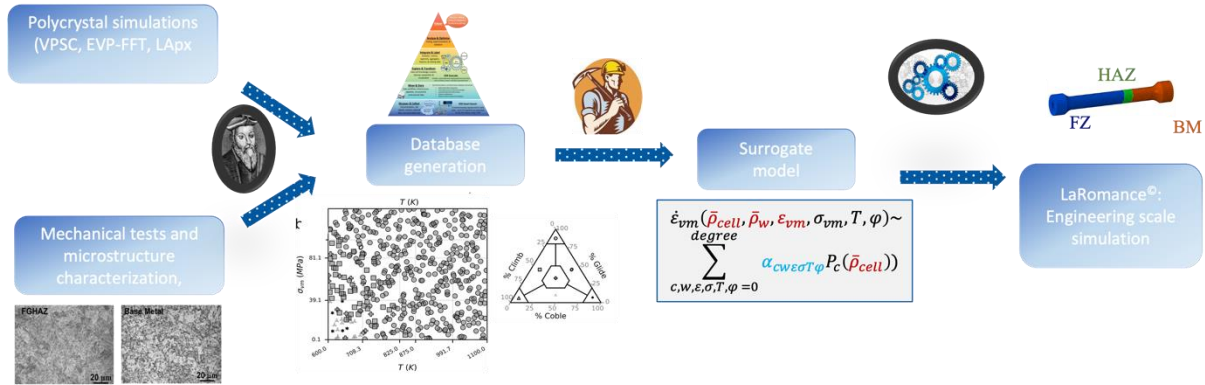


Figure 63. Computational Flowchart Showing How LAROMance Models are Developed

#### 5.3.4.2 Data Collection and Transfer

LAROMance mines large databases of the predicted response of polycrystals. These are typically generated using LApX. These databases record as a function of time, the evolution of all internal state variables of the model and of the associated/connected mechanical response. In total an input database used train LAROMance will reach sizes in the range of 100 Mb. Once trained, a LAROMance type model will consist of a finite element level subroutine accompanied by a series of fitted parameters (Legendre interpolation coefficients) thus totaling less than 20kb of memory.

#### 5.3.4.3 Data Visualization and Analysis

NA

## 6.0 Experimental Equipment and Simulation Tools: ORNL

### 6.1 Advanced Manufacturing Technologies

#### 6.1.1 Renishaw AM 250

##### 6.1.1.1 Overview

The Renishaw AM 250 is a single-laser, Laser Powder Bed Fusion printer with a build volume of 250 mm × 250 mm × 365 mm (Figure 64). This Additive Manufacturing operation acts on powdered metal feedstock and may instantiate new parts within the Digital Platform in the future. The MDF typically prints a wide range of metal alloys on this system.



Figure 64. RenishawAM250-008W73 Single-Laser, Laser Powder Bed Fusion Printer

Table 44. Metadata Information for RenishawAM250-008W73 Single-Laser, Laser Powder Bed Fusion Printer

Category	Value
Digital Platform Tag(s)	RenishawAM250-008W73
Digital Point of Contact	
Approximate Data Volume per Operation (GB)	50 per layer
Approximate Number of Operations per Year	20
Associated Software Tools	Peregrine

### 6.1.1.2 Data Collection and Transfer

Peregrine is installed at the edge on a local compute node with a user display (desktop computer on a rolling cart). The Peregrine computer is able to communicate with the printer control computer through WinSCP, open-source SSH File Transfer Protocol, allowing the Peregrine computer to directly access folders on the printer control computer to distribute build files and retrieve log files. The Peregrine computer is connected via USB to cameras (a 20 MP Basler - acA5472-17um and a 4.2 MP Pixelink - PL-D734MU-NIR-T), which observe the powder bed and automated analysis of the live video stream is used to trigger layer-wise image capture. Each layer-wise image is then stored on the Savitar file storage system and the edge instance of Peregrine locally analyzes the data using the neural networks and collates the data for the entire build. After the build is complete, the operator loads the log file onto Savitar via the edge Peregrine instance. Metadata are entered into either Peregrine or the Digital before, during, and after each build.

### 6.1.1.3 Meta data

Figure 65 provides an overview of the Peregrine metadata manager interface. The information listed on this page is recorded in the SQL database in multiple tables.

Metadata Manager

<b>MDF printer tag</b>	<b>customers</b>	<b>Charge Code</b>	<b>Beam Calibration Date</b>
RenishawAM250-008W73			
<b>build name</b>	<b>material type</b>	<b>Powder Use Cycles</b>	<b>Data Restrictions</b>
Data Acquisition Test (not	none		
<b>build date</b>	<b>feedstock batch</b>	<b>Wiper Uses</b>	
2023-03-30	none / none / none		
<b>tracking ID</b>	<b>operator #1</b>	<b>Build Volume</b>	
	Zackary Snow	full	
<b>data are sensitive</b>	<b>operator #2</b>	<b>Base Plate Size</b>	
False	Zackary Snow	248x248mm	
<b>layer thickness (mm)</b>	<b>amb. humidity (RH%)</b>	<b>Base Plate Material</b>	
0.03			
<b>global scan rotation (°/l)</b>	<b>amb. temperature (°C)</b>	<b>Total Powder Volume (ccm)</b>	
67.0			
<b>projects</b>	<b>qual. build quality [0-3]</b>	<b>Expected Build Time (h)</b>	
Advanced Materials and M			

**design and documentation files**

**build info**

In-Situ and Process Data Checklist (X)

- ✓ Camera calibration
- ✓ Layer-wise powder bed images
- X Part templates
- X Sample templates
- ✓ Collated build analysis
- X Log files
- X Scan paths
- X Design and documentation files
- X Reference images
- X Process parameters

Ex-Situ Data Checklist

- X Property test results
- X Registered or characterization data
- X Micrographs

**build notes**

Not a real build, just simulating a real build to test the data acquisition system's stability for long layer times. Note: the buffer for the temporally integrated images is 6000 frames (5 fps \* 60 seconds \* 10 minutes \* 2)

230330 - 10:30am: Starting with 2 minute simulated layers, it takes about 50-55 seconds for the sensor images to show up in the build's Peregrine data folder. Will let it run for a few hours and then switch to 8 minute simulated layer times to assess how long it will take to generate the temporally integrated images.

230330 - 11:45am: After 36 layers of data collecting, it takes about 55 seconds for the sensor images to show up in the build's Peregrine data folder. Therefore, no buildup of data processing and timings appear to be good. Stopping data acquisition and switching to 15 second layer times to see if the cycle time drops appropriately.

230330 - 11:50am: For 15 second layer times, it takes approximately 4

**Save** **Cancel** ☐ certify that all in-situ and process data are uploaded





   

Figure 65. Peregrine Metadata Manager for the Renishaw AM 250

Most of the fields on this form are self-explanatory; however, we are providing more details in Table 45 for few of them.

Table 45. Metadata Information for Renishaw AM 250 Printer

Field name	Metadata Information	DB Table	DB Key	Is list?
MDF Printer Tag	Unique name identifier for the machine, concatenating the machine type and the serial number. Can be used for keyword search using the platform application programming interface.	machine_info	machine_name	No
Customers	Provide the list of the customers for any given build. More than one customer can be listed as the build chamber allows for multiple components to be manufactured simultaneously	build_info	customer_ids	Yes
Charge code	Provide the list of the charge numbers used for any given build. Multiple change numbers can be listed if different project support a particular build	build_info	chargecode_ids	Yes
Beam calibration date	This is a foreign key to machine_info table that list of all laser calibration dates for the machine. Each build only list one date.	build_info	calib_date	Yes
Build name	Name given to the build by the operator of the machine for identification.	build_info	Build_name	No
Material type	Type of material used for this build. The name is store in a separate table specific to the type of material (in this case the table named <i>powder</i> , field <i>composition</i> ). This is a foreign key to materials table	build_info	material_id	No
Powder use cycles	(In progress) provide the material cycle history for the batch of powder used for this build. This is a foreign key to materials table	build_info		
Data restrictions	Indicate the sensitivity of the data between the following options: open, EC, ITAR, and industry confidential	build_info	sensitivity_type	No
Build date – start		build_info	start_date	No
Build date – end		build_info	end_date	No
Feedstock batch		build_info		
Wiper uses		build_info		
Tracking ID		build_info		
Operators #1	Provides the name of the operator involved in the <u>start-up</u> of the build. This is a foreign key to users table	build_info	startup_tech_id	No
Operators #2	Provides the name of the operator involved in the <u>setup</u> of the build. This is a foreign key to users table	build_info	setup_tech_id	No
Build volume	Provide the build volume for the build. The value will change between builds	build_info		

Field name	Metadata Information	DB Table	DB Key	Is list?
	based on the size of the printed object. The machine_info table however will list the maximum build volume for the machine			
Base plate size	Provide the dimensions of the base plate used for this build. In certain cases, different build plate can be used at the discretion of the operator. The machine_info table however will list the maximum build plate size for the machine	build_info		
Base plate material		build_info		
Data are sensitive	Boolean to simplify access control to sensitive data	build_info	is_sensitive	No
Layer thickness		build_info		
Global scan rotation	Provide the angular rotation of the scan strategy traditionally used to reduce defect during manufacturing. This angle varies based on the combination geometry complexity, material, and process parameters. Changes are usually driven by execution experience and/or scientific choices	build_info		
Ambient humidity		build_info		
Ambient temperature		build_info		
Total powder volume	Total quantity of powder used to complete the build.	build_info		
Projects	Provide the list of projects for any given build. More than one projects can be listed as the build chamber allows for multiple components to be manufactured simultaneously	build_info		
Qual. build quality		build_info		
Expected build time	Indicate the calculated build time from the selected process parameters			
Build notes	Text field to record comments/notes by technicians of the build	build_info	comments	No

#### 6.1.1.4 Powder Bed Imaging

A 20-MP grayscale camera (Basler - acA5472-17um), sensitive in the visible spectrum, captures an image of the entire print area immediately after powder fusion and after powder spreading for each layer. A 4.2-MP camera (Pixelink - PL-D734MU-NIR-T) captures temporally integrated thermal images of the entire build area, resulting in three images: 1) integrated sum, 2) integrated max, and 3) integrated time-of-max. Both systems were designed and installed by ORNL. Anomalies observable with this system include damage to the recoating mechanism, improper spreading of the powder, swelling or distortion of the part geometry, damage to the as-

printed components, abnormal generation of spatter and other melt pool ejecta, and improper fusion of the powder.

In the case of a high-speed video monitoring, the data transfer requirement do not allow for direct recording to the hard disk drive of a standard edge system. In this case a computer was custom designed to allow for such data transfer with the intent to develop processing algorithms for real time data compression and recording, or real time data analytics. In both cases the RAW data, respectively due to data compression loss and data conversion, i.e., the RAW data will not be recorded but immediately processed and converted into analytical results that can be recorded.)

#### **6.1.1.5 Machine Health Data**

At the end of each build, a log file is produced, which reports various machine error states as well as temporal sensor streams including build chamber gas (argon) flow rates, build chamber oxygen concentrations, powder roller loading conditions, and the temperatures of selected components in the laser optic trains. This system is installed and maintained by Renishaw, and the resulting log files are loaded into Peregrine at the end of each build.

#### **6.1.1.6 Data Visualization and Analysis**

In-situ data analyses are currently performed by the Peregrine Software Tool, as well as embedded versions of the SWAN and Pterodactyl packages.

## **6.2 Mechanical Testing and Material characterization Equipment**

### **6.2.1 X-Ray Computed Tomography: METROTOM**

#### **6.2.1.1 Overview**



Figure 66. RenishawAM250-008W73

Table 46. Metadata Information for Renishaw AM 250

Category	Value
Digital Platform Tag(s)	-
Digital Point of Contact	Amir Ziabari
Approximate Data Volume per Operation (GB)	8–15
Approximate Number of Operations per Year	1,000
Associated Software Tools	Cera (ZEISS Reconstruction software), GOM Volume Inspect, VGStudio, IC3D

#### 6.2.1.2 Data Collection and Transfer

Currently, ex situ data is manually retrieved from the METROTOM using an un-encrypted hard drive. This hard drive is then hand-delivered to one or more desktop computers located inside or outside of the EC office space. Data are currently stored in an un-centralized manner by Principal Investigators. Metadata is currently not tracked but is available provided OEM files are maintained.

#### 6.2.1.3 Imaging

A 2-K X-ray detector (size: 1840 × 1456 pixels) were installed, and are maintained, by Zeiss. It is an industrial computed tomography system for measuring and inspecting complete components made of plastic or metals. It avoids the challenges associated with traditional measuring technology, that can inspect hidden structures only after the time- and cost-consuming process of destroying the component layer-by-layer. At the MDF, the system has been mainly used for defect/pore detection, metrology, among other applications.

#### 6.2.1.4 Data Visualization and Analysis

The analysis software GOM Volume Inspect is being used for complete CT data analysis in three dimensions. Geometries, shrinkage holes or internal structures and assemblies can be analyzed precisely. Defects become visible through individual sectional images and can be automatically evaluated according to various criteria. Volumetric data of several components can be loaded into a project, perform a trend analysis and compare the analysis with CAD data, which is beneficial to determine and document the quality of the component. Cera is the main software being used by the system for image reconstruction from the 3-D raw projection volume. IC3D is being developed by ZEISS and frequently being tested on the parts being manufactured at the MDF for image analysis applications such as segmentation, detection, registration.

The MDF digital team is developing artificial intelligence-based Simurgh software that allows for fast and very high-quality reconstruction of metal additive manufactured parts. Leveraging CAD models of the parts along with physics-based information, the software allows for significant improvement for defect detection (3X so far) and resolution, while reducing the scan time (4× so far).

### 6.2.2 XRADA VERSA 620

#### 6.2.2.1 Overview



Figure 67. XRADA VERSA 620

Table 47. Metadata Information

Category	Value
Digital Platform Tag(s)	-
Digital Point of Contact	Amir Ziabari
Approximate Data Volume per Operation (GB)	15–20
Approximate Number of Operations per Year	750
Associated Software Tools	Dragonfly, ZEISS reconstruction software, IC3D,

#### 6.2.2.2 Data Collection and Transfer

Currently, ex-situ data is manually retrieved from the Xardia Versa using an un-encrypted hard drive. This hard drive is then hand-delivered to one or more desktop computers located inside or outside of the EC office space. Data are currently stored in an un-centralized manner by Principal Investigators. Metadata is currently not tracked but is available provided OEM files are maintained.

#### 6.2.2.3 Imaging

The Xradia Versa family of submicron X-ray microscopes uses patented X-ray detectors within a microscope objective turret to enable increased magnification on various sample types and sizes with spatial resolution down to 500 nm. The system provides high resolution across a broad range of sample types, sizes, and working distances. It can also provide in situ imaging for non-destructive characterization of microstructures in controlled environments and over time (stop and shoot 4DCT). Akin to other X-ray CT systems, this avoids the challenges associated with traditional measuring technology, that can inspect hidden structures only after the time- and cost-consuming process of destroying the component layer-by-layer. At the MDF, the system has been mainly used for high resolution defect/pore/void and high-z inclusion detection,

metrology, as well as for detailed shape, size, and volume distribution analysis of powder bed particles to determine proper process parameters.

#### **6.2.2.4 Data Visualization and Analysis**

The Scout-and-Scan software is being used for reconstruction of the measured X-ray CT data. It also allows for easily scouting a region of interest and specify scanning parameters within the Scout-and-Scan Control System. Further, it can be used for aligning multi-resolution scan of the same part and better characterization of defects in additive manufacturing. In addition, the Dragonfly Pro from ORS is being used for analysis and visualization of 3-D data acquired by the system. Available exclusively through ZEISS, ORS Dragonfly Pro offers a toolkit for visualization and analysis of large 3-D grayscale data. Dragonfly Pro allows for navigation, annotation, creation of media files, including video production, of the 3-D data. It can also be used to perform image processing, segmentation, and object analysis to quantify your results. The MDF digital team is developing artificial intelligence-based Simurgh software that allows for fast and very high-quality reconstruction of metal additive manufactured parts. The software allows for significant improvement for defect detection (3× so far) and resolution, while reducing the scan time (4× so far).

## 7.0 Conclusions and Recommendations

This report outlines prospective data streams originating from PNNL's, INL's, ANL's, LANL's and ORNL's manufacturing, characterization, and modeling tasks that could potentially integrate into the MDDC framework as part of the AMMT program endeavors. The document elucidates the nature of the data, data collection process, and resulting storage requirement for the generated data. Based on the current data stream framework, PNNL, INL, ANL, LANL and ORNL will introduce similar types of frameworks for any new manufacturing, characterization, or models introduced in the future under AMMT project spaces to integrate into the MDDC. While the current data template provides a foundation with general equipment-related information, a forward-looking approach entails the development of customized reporting mechanisms for each distinct equipment and software. This comprehensive approach entails capturing an exhaustive range of data and metadata specific to the respective tools and software. To facilitate this seamless integration of data streams into the MDDC framework, it is envisioned that each member actively engaged in the AMMT initiative will generate new MDDC data stream reports for every newly developed data stream. A logical next step for this work is to integrate the MDDC framework into PNNL's, INL's, ANL's, LANL's and ORNL's fabrication, experimentation, and modelling work flows. This would require setting up the MDDC framework at PNNL, INL, ANL and LANL and integrating it into the data collection and storage for these different activities. Over time, this data might be shared across multiple labs contributing to the AMMT program to make a larger dataset available to develop and understanding of how material processing conditions and microstructure influences critical material properties.

## 8.0 References

- [1] Lindsay et al. “2.0 – MOOSE: Enabling massively parallel multiphysics simulations.” Software X 20, pp. 101202, 2022.
- [2] Schoof, Larry A. and Victor R. Yarberr. “EXODUS II: A Finite Element Data Model.” Sandia National Laboratories technical report SAND92-2137/UC-705, 1994.
- [3] Roters, Franz, et al. “Crystal plasticity finite element methods: in materials science and engineering.” John Wiley & Sons, 2011.
- [4] Bradbury, et al. “JAX: composable transformations of Python+NumPy programs.”

# **Pacific Northwest National Laboratory**

902 Battelle Boulevard  
P.O. Box 999  
Richland, WA 99354

1-888-375-PNNL (7665)

***[www.pnnl.gov](http://www.pnnl.gov)***